3D Fractals

Dominic Rochon*

UNIVERSITÉ DU QUÉBEC À TROIS-RIVIÈRES

May 2006

***Research supported by CRSNG (Canada)**

Outline

I. The Birth of Fractals

II. Bicomplex Dynamics

III. Bicomplex Distance Estimation

The Birth of Fractals

Dominic Rochon*

(Joint project with Josiane Lajoie)

UNIVERSITÉ DU QUÉBEC À TROIS-RIVIÈRES

May 2006

***Research supported by CRSNG (Canada)**

Outline : The Birth of Fractals

1. In the beginning
2. The mathematical crisis
3. About dimensions
4. The birth of fractal geometry
5. More about fractals

IN THE BEGINNING

- First fractal images
  - Apollonius of Perga
  - Albretch Dürer
- Self similarity (Leibniz)

The Apollonian Gasket
(300 B.C.)

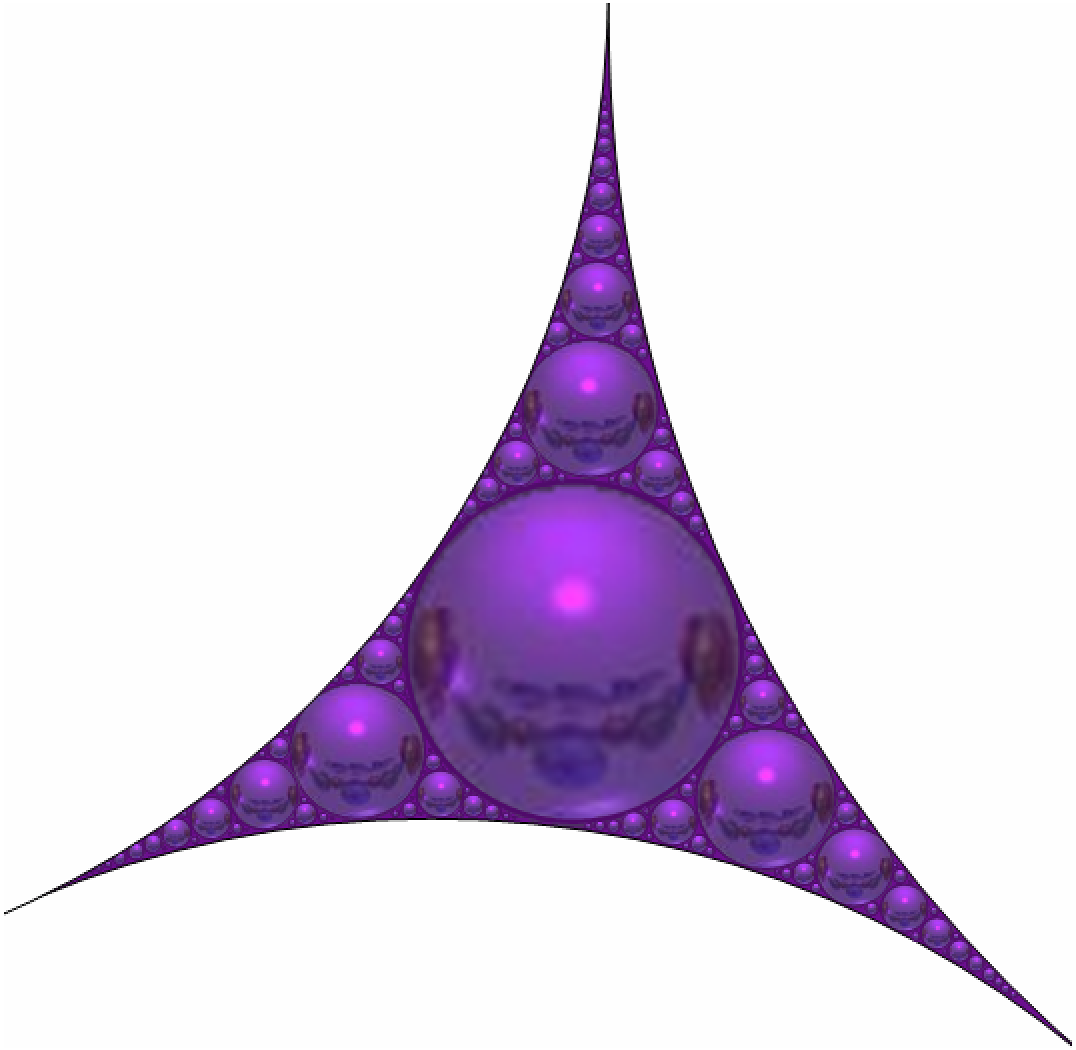

Dürer Pentagon (1520)

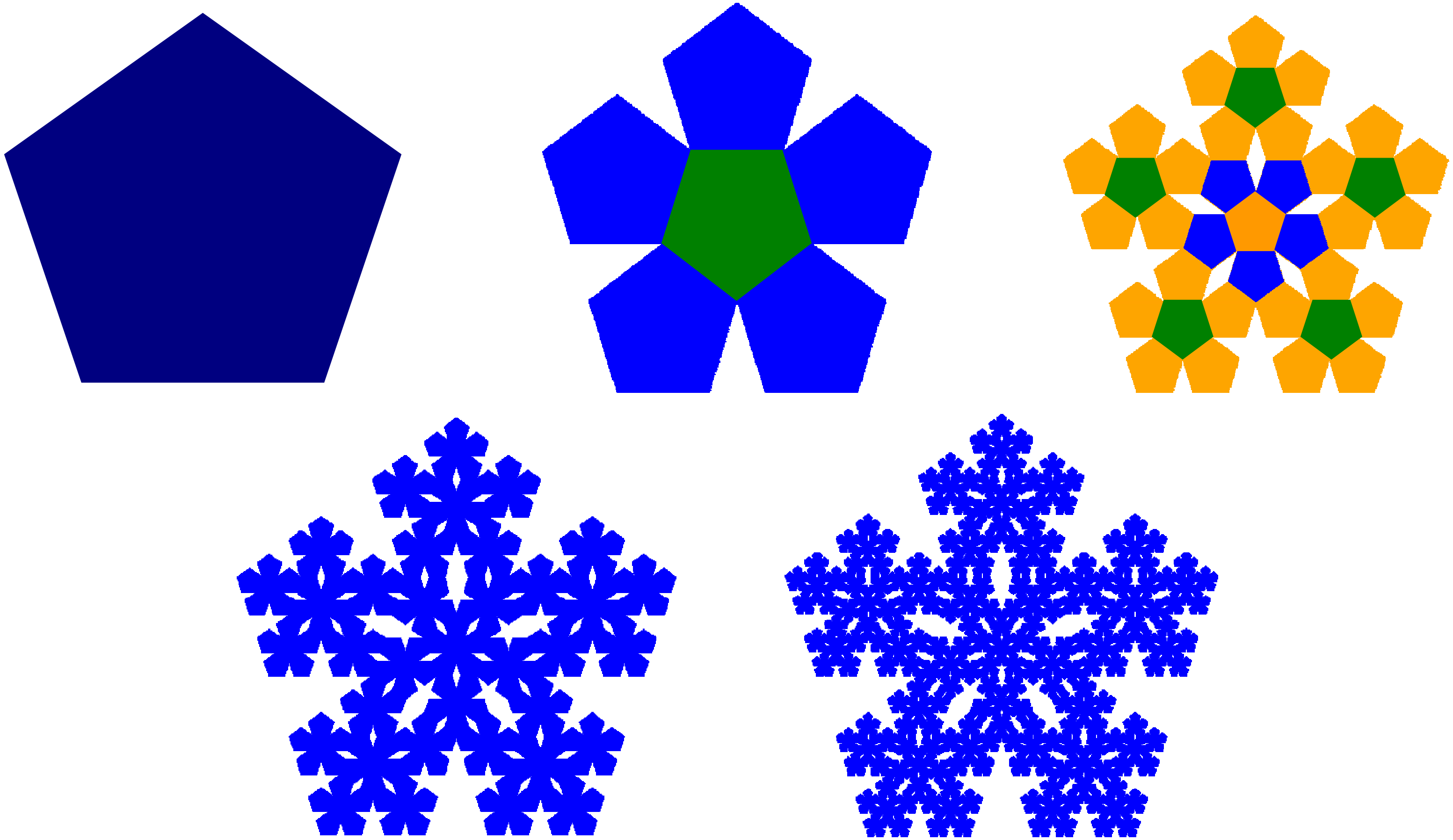

THE MATHEMATICAL CRISIS

- 1875 to 1925
- "Pathological Monsters"
- Begins with Karl Weierstrass
  - Study of complex functions
  - A non-differentiable continuous curve!

Helge von Koch

- Recall: Weierstrass (1875) showed an example of a non-differentiable continuous curve.
- Helge von Koch (1904) suggested a simple construction of a continuous curve without a tangent.

Koch Curve (1904)

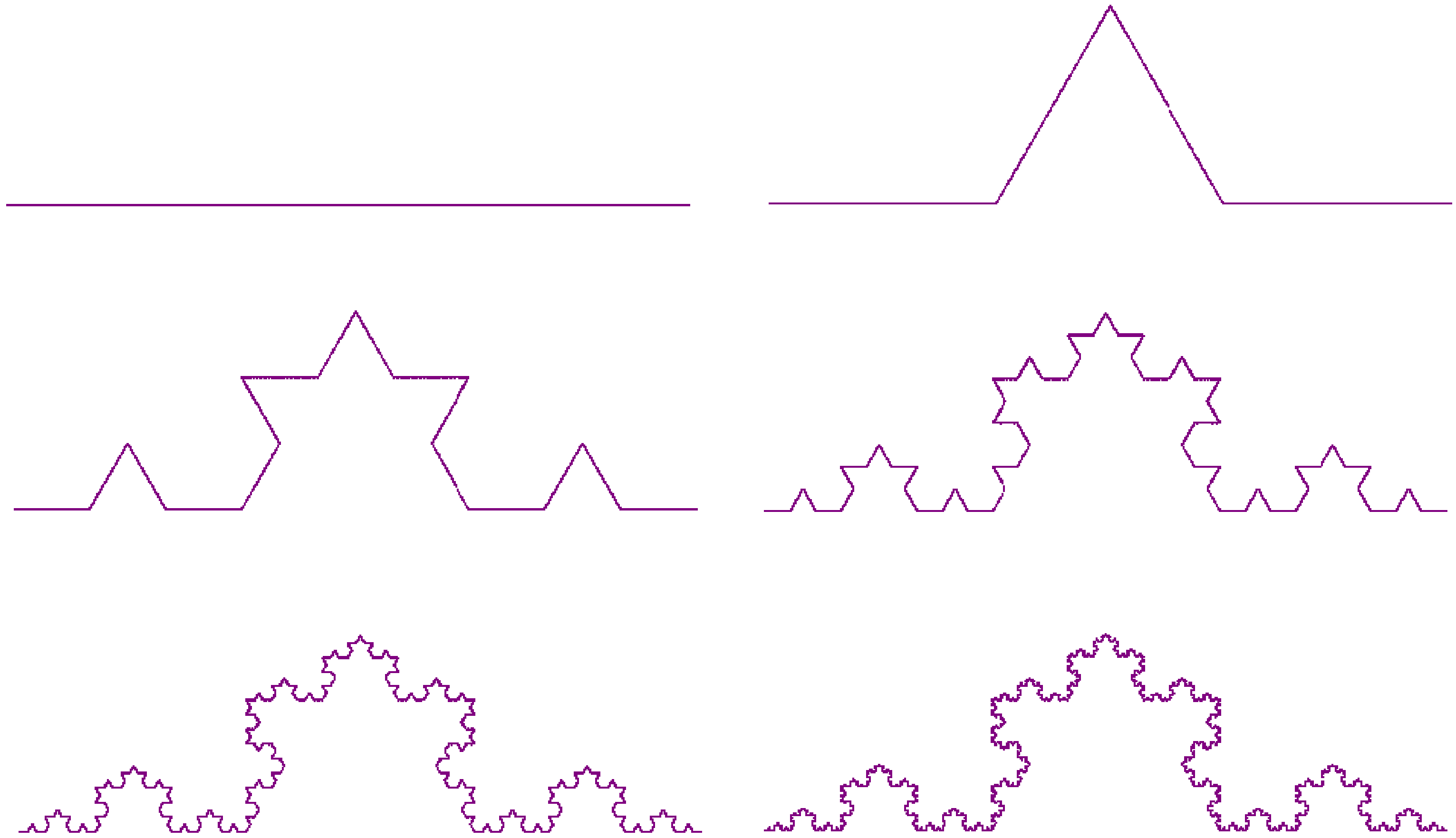

Waclaw Sierpinski

Waclaw
Sierpinski

- Sierpinski gasket

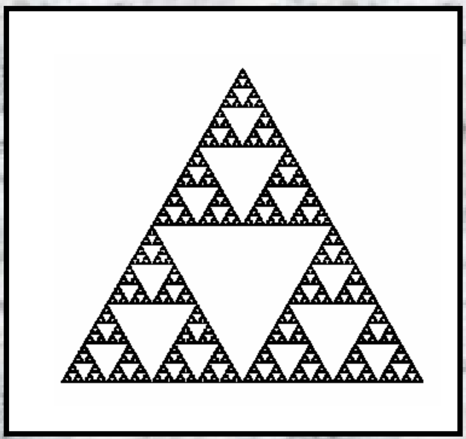

- Generalization to all n sided polygons.

Sierpinski Polygons

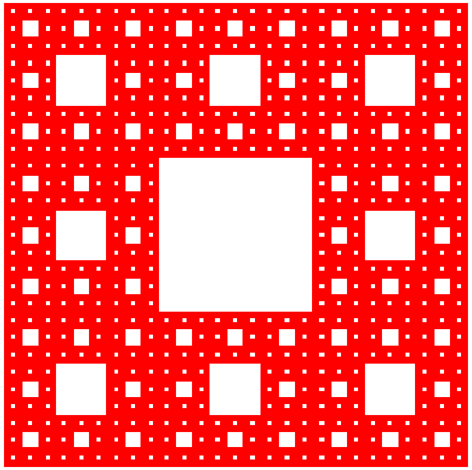

Sierpinski square

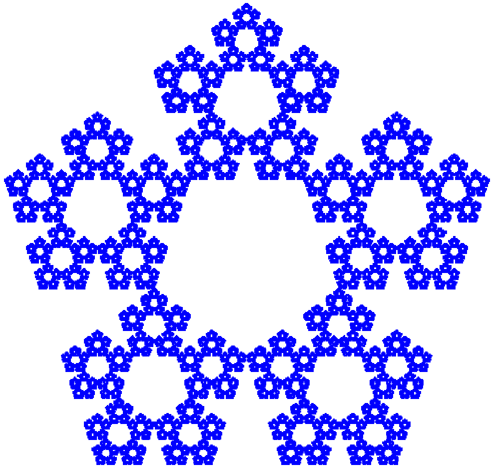

Sierpinski pentagon

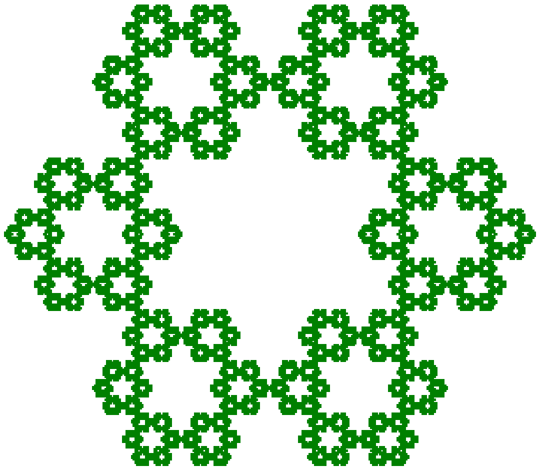

Sierpinski hexagon

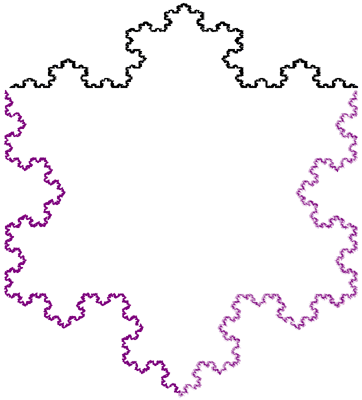

Koch curve

3D Sierpinski

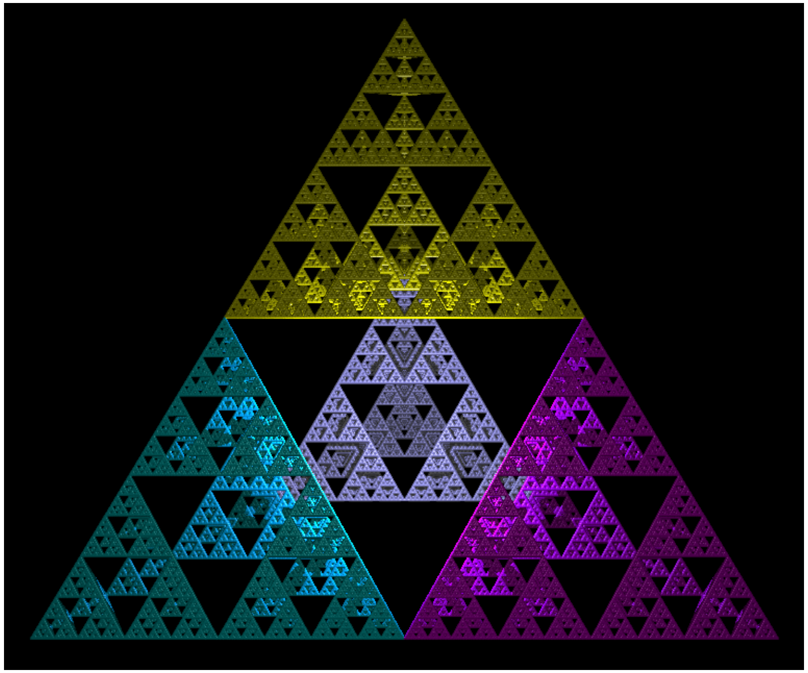

Sierpinski pyramid

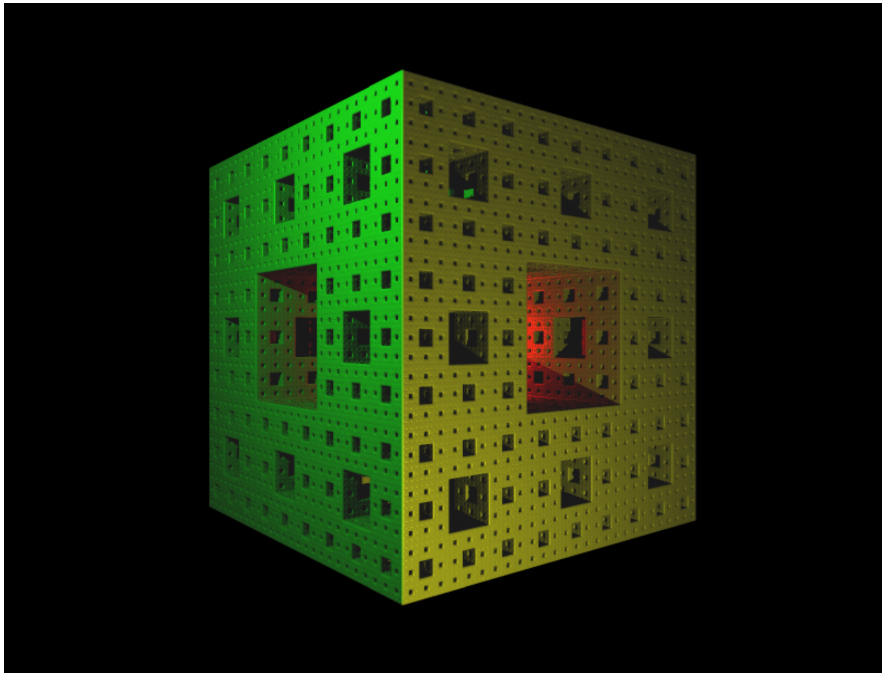

Menger – Sierpinski sponge

Source: http://fractals.nsu.ru/gallery_en.htm

ABOUT DIMENSIONS

- First definition: Euclide (*The Elements*)
- Problem: transformation from $[0,1]$ to the square.
- Some definitions were suggested
- Two types of dimension:
  - Integer values (topologic)
  - Real values: Hausdorff (1919), Bouligand-Minkowski (1929), Richarson (1960), Tricot (1982), …

Box-counting Dimension

- Seems that it was developped by Hausdorff's followers (around 1930)
- Idea:
  - Cover the figure with boxes of ε-length sides.
  - Determine the smallest number of boxes needed, in function of ε noted $N(\varepsilon)$.
  - Calculate the dimension using the following formula:

$$\lim_{\varepsilon \to 0} \left(\frac{\log N(\varepsilon)}{\log(1/\varepsilon)} \right)$$

Box-Counting Dimension of the Sierpinski Gasket

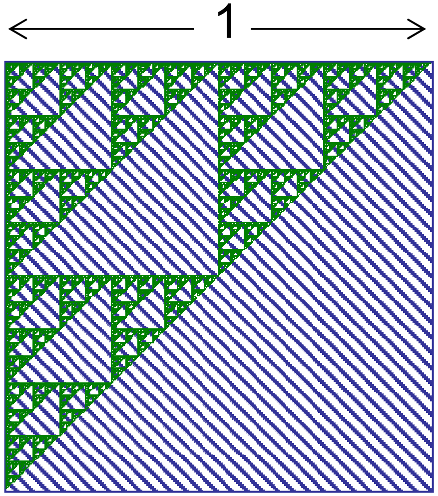

$\varepsilon = 1$

$N(\varepsilon) = 1$

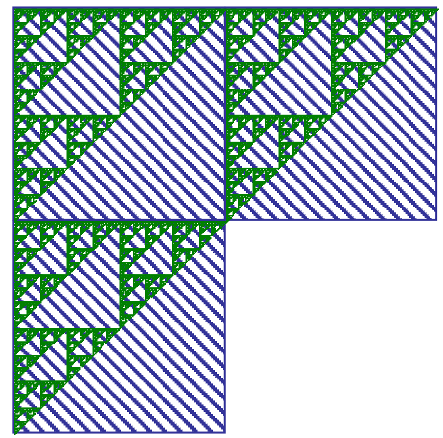

$\varepsilon = ½$

$N(\varepsilon) = 3$

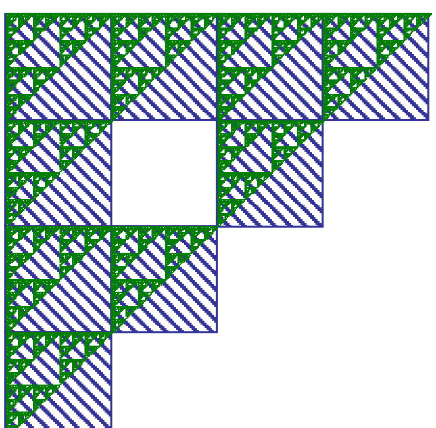

$\varepsilon = ¼$

$N(\varepsilon) = 9$

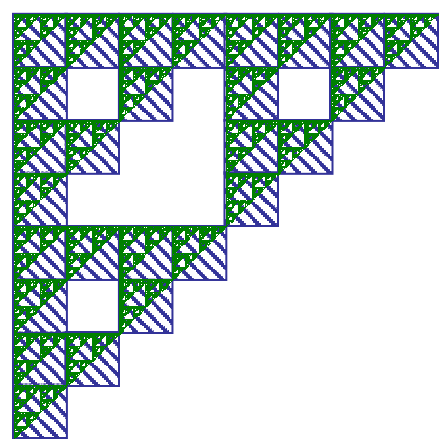

$$\varepsilon = \frac{1}{2^n}$$

$$N(\varepsilon) = 3^n$$

d'où

$$d = \lim_{n\to\infty}\left(\frac{\log 3^n}{\log 2^n}\right) = \frac{\log 3}{\log 2}$$

Coasts Length

- Richarson brought the problem of the coasts' length. As an example:
  - – Coast length between Spain and Portugal: 616 milles (Spain) or 758 milles (Portugal)
- Coast length goes to infinity!

Britain Coast Length

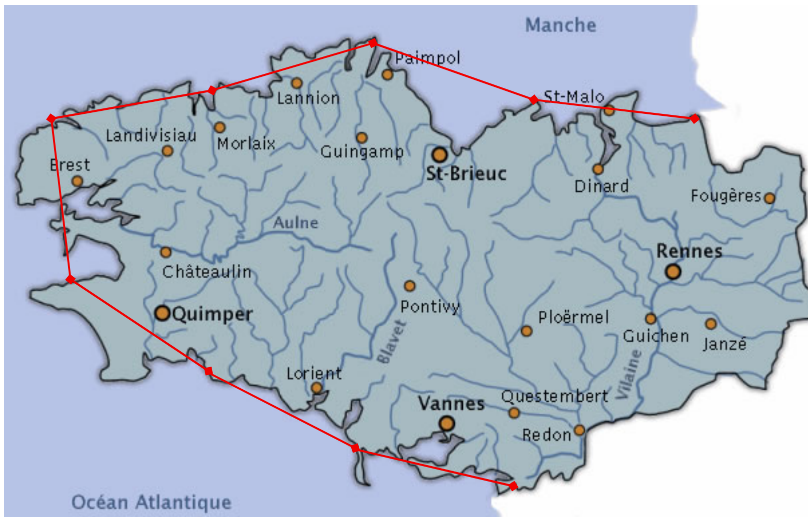

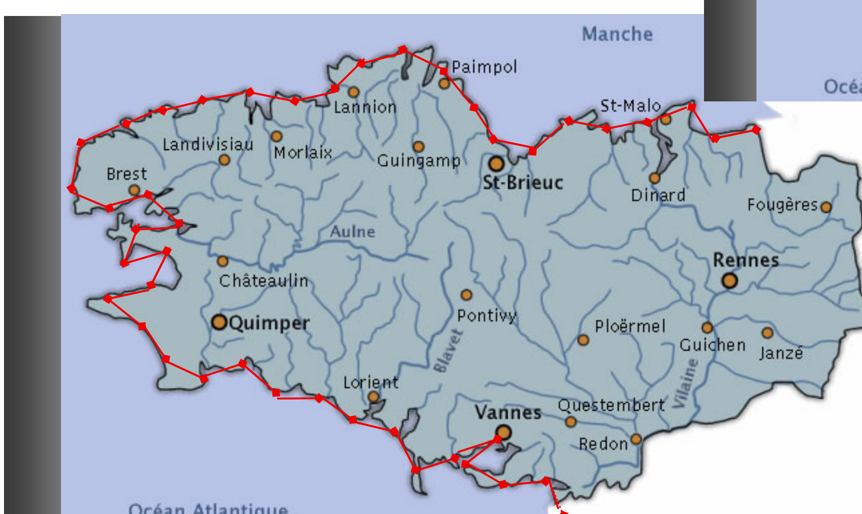

THE BIRTH OF FRACTAL GEOMETRY

- So, we have:
  - Difficultly describable physics phenomenons;
  - "Pathological Monsters".
- Mandelbrot's idea:
  - Name those objects;
  - Study their communal properties.
- Creation of the word "fractal" (1975) whose root means "broken" and "irregular".

Fractal Definition

- Different definitions depending of the authors.
- Mandelbrot: "*A fractal set (in a plane or in space) is a set for which its Hausdorff-Besicovitch dimension is stricly greater then its topologic dimension.*"
- Fractal caracteristics:
  - Its parts have approximately the same structure as the whole;
  - Its form is extremly irregular or fragmented;
  - It contains new details on a large scaling range.

Another Contribution

- Mandelbrot noticed that fractals are everywhere in nature:
  - Clouds are not spheres;
  - Mountains are not cones;
  - Islands are not circles;
  - …

- Natural elements description need an adapted geometry.

MORE ABOUT FRACTALS

- There are different kinds of fractals.
- Some ways to make fractals:
  - Complex iterations
  - Iterated functions system (IFS)
  - L-systems

Complex Iterations

- Julia (1918) suggested to iterate the complex polynomial $z_{n+1} = z_n^2 + c$ for a constant number c.
- The filled-Julia set associated to c (K_c) is formed by the points z who generate a bounded sequence.
- The boundary of the filled-Julia set is the Julia set (J_c).
- The arrival of computers allowed us to visualize those images.

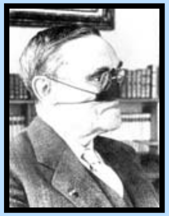

Gaston Julia

Filled-Julia Sets Associated to the Point c

Louis Fatou

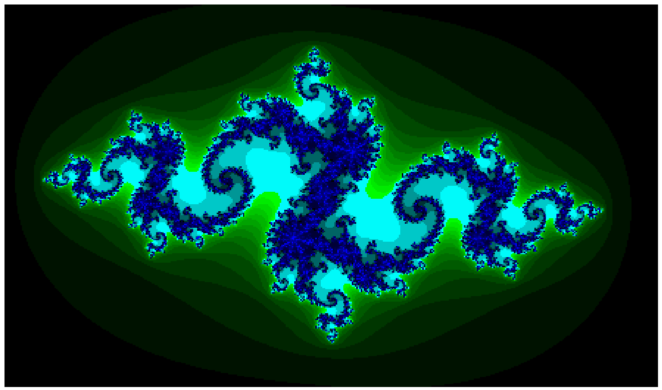

c = -0.8+0.168i

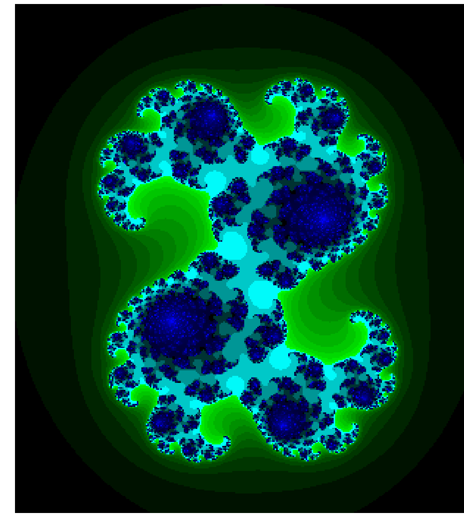

c = 0.328+0.048i

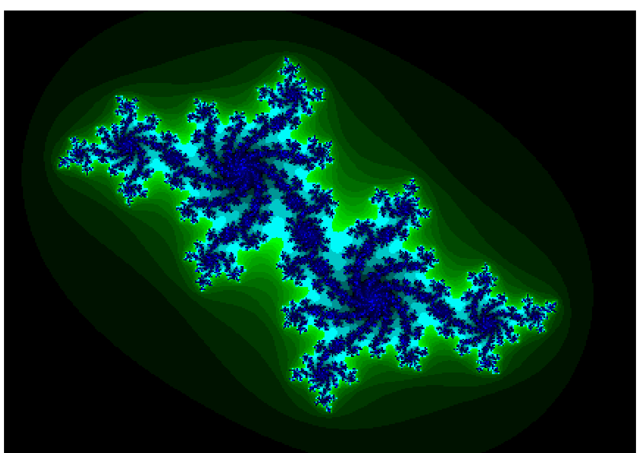

c = -0.344+0.64i

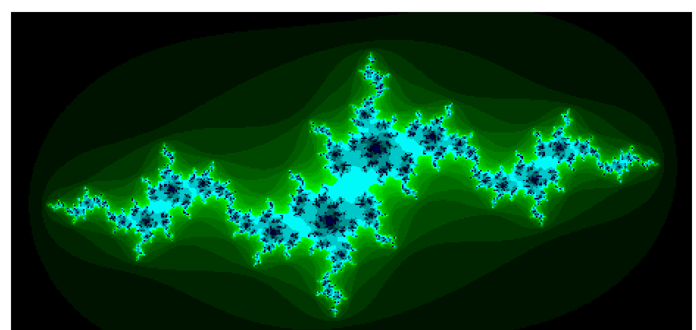

c = -1.096-0.264i

Mandelbrot Set

- M = $\{c \in \mathbb{C}: J_c$ is connected$\}$
- We can generate the Mandelbrot set with the same polynomial $z_{n+1} = z_n^{\,2} + c$. This time we fix $z_0 = 0$ and we iterate for each complex number c.

Mandelbrot Set

Benoit Mandelbrot

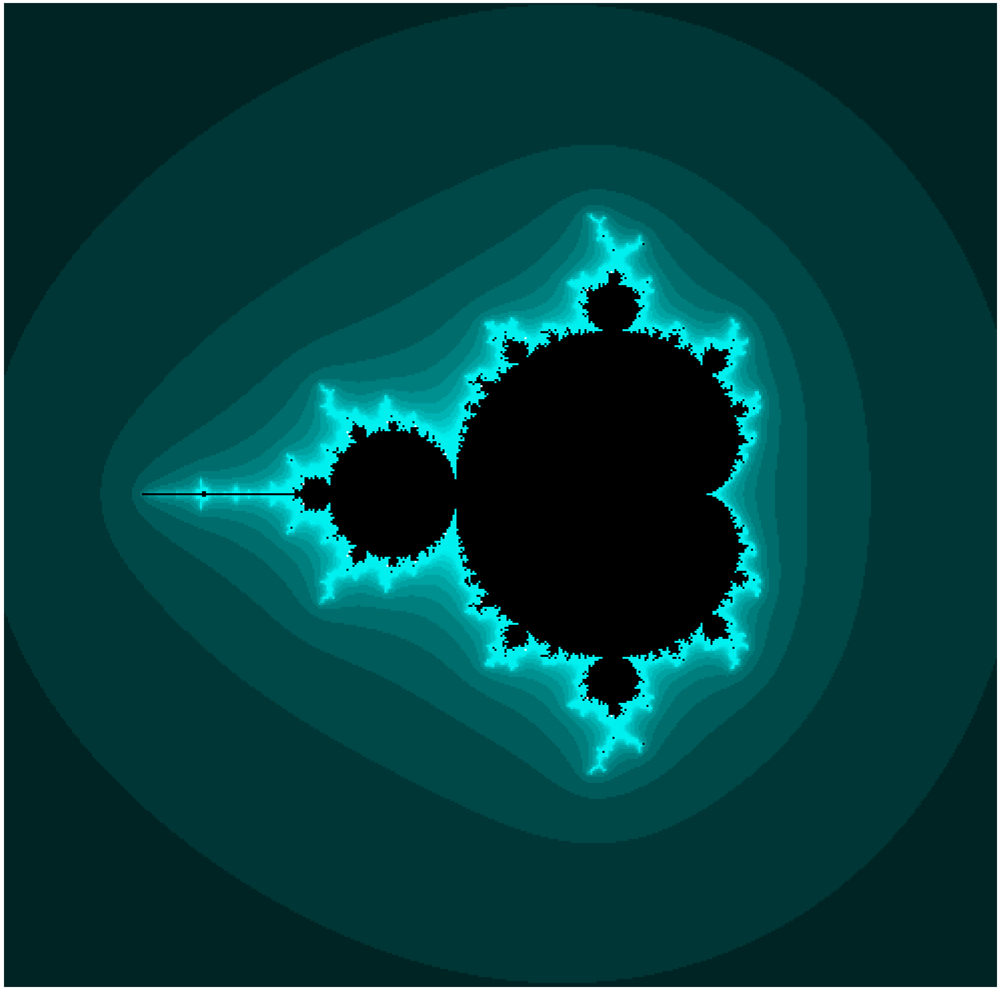

Iterated Functions Systems (IFS)

- These iterations converge to a final image called "attractor" of the functions system.
- Theory is based on the Banach fixed point theorem. So,
  - The attractor exist;
  - The attractor is unique, no matter which starting figure is chosen.

Example of Fractal Construction Using IFS

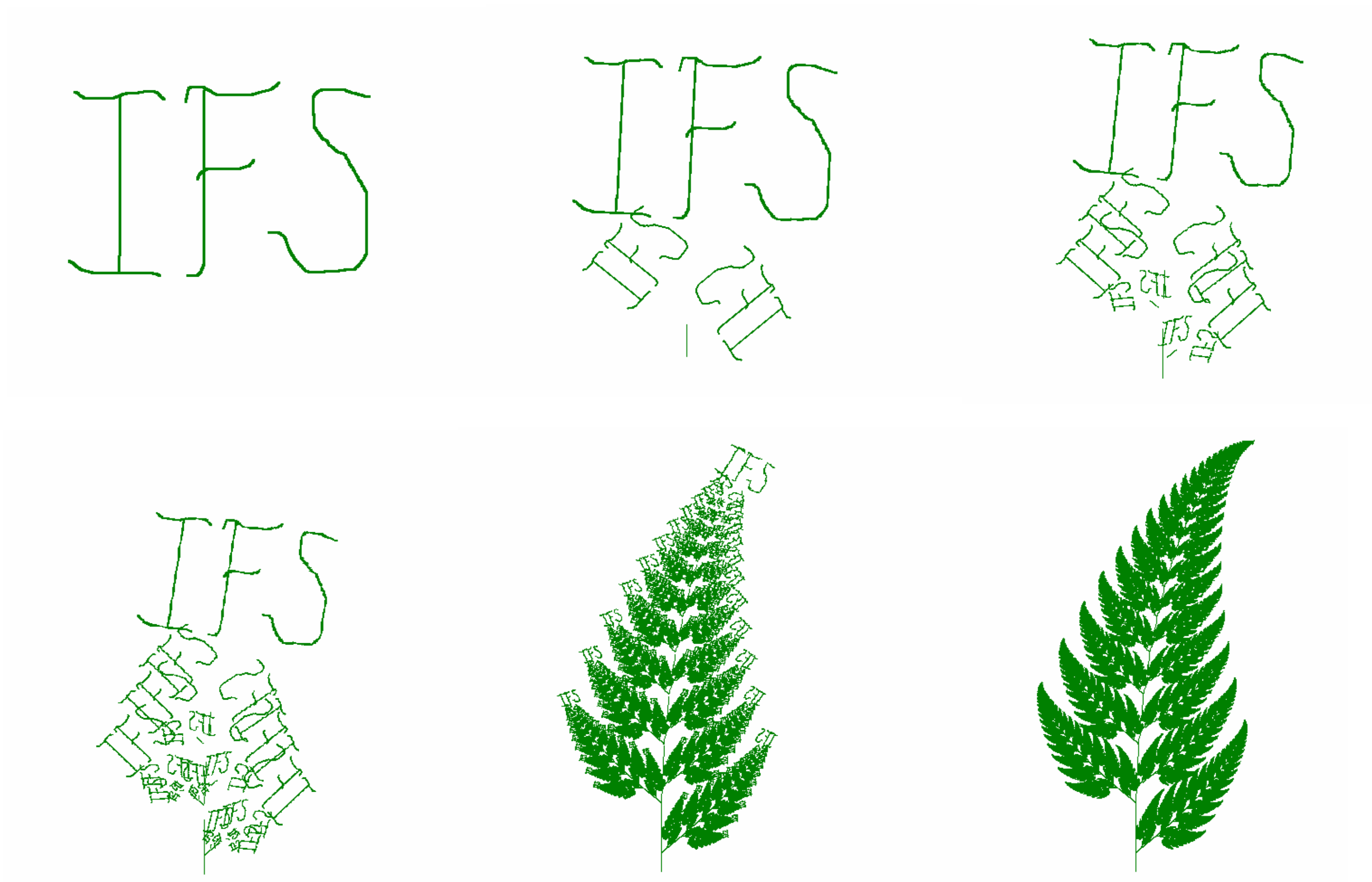

L-Systems

- Aristid Lindenmayer (1968) formally described plant-growth.
- He used a character-string to describe a figure.
- Recursive process

Example of a L-system

L-system:	Plant
Axiom:	*F*
Production rule:	$F \rightarrow F[+F]F[-F]F$
Parameter:	$\theta = 25{,}7^o$

Axiom:

F

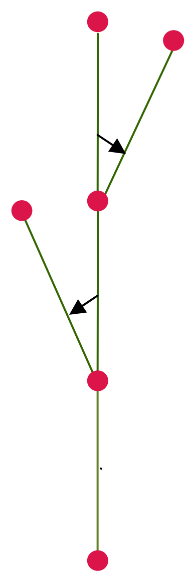

Step 1:

$F\,[\,+\,F\,]\,F\,[\,-\,F\,]\,F$

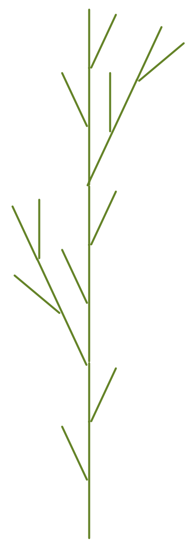

Step 2:

$(F[+F]F[-F]F)\ [+(F[+F]F[-F]F)](F[+F]F[-F]F)[-(F[+F]F[-F]F)](F[+F]F[-F]F)$

…

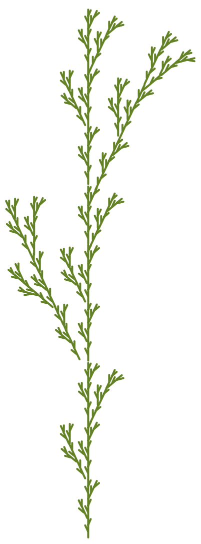

Step 4:

…

Chronological Summary

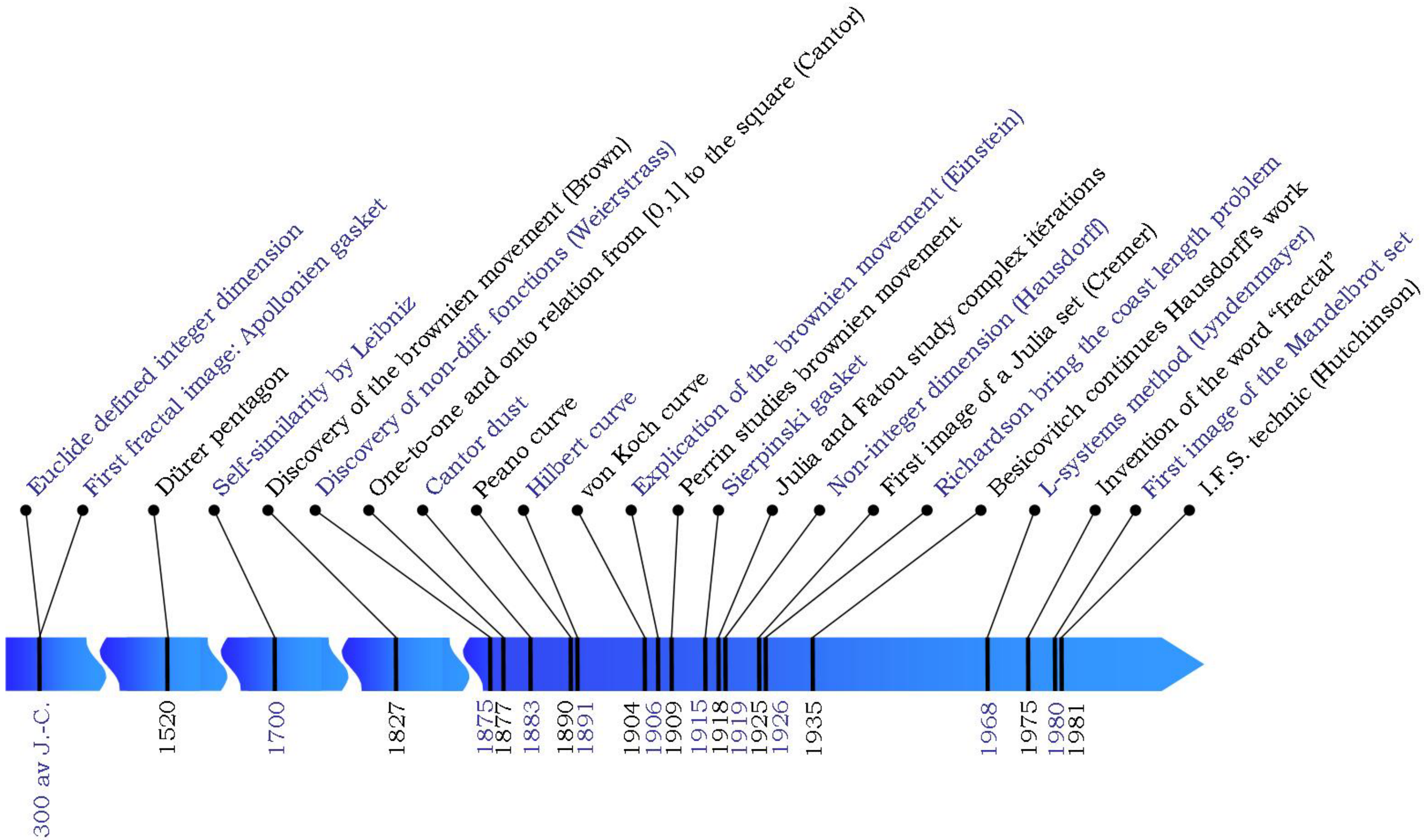

Bicomplex Dynamics

Dominic Rochon*

UNIVERSITÉ DU QUÉBEC À TROIS-RIVIÈRES

May 2006

---

*Research supported by CRSNG (Canada).

Outline : Bicomplex Dynamics

- Bicomplex Numbers
- Bicomplex Dynamics
  - Bicomplex Mandelbrot Set
  - Bicomplex Filled-Julia Sets
  - Definition of the Tetrabrot
- Generalized Fatou-Julia Theorem
  - Strong Basin of Attraction of ∞
  - Cantor Sets in $\mathbb{R}^4$
- Bicomplex Filled-Julia Sets in $\mathbb{R}^3$

Quaternionic Dynamics

- In 1982, A. Norton gave some straightforward algorithms for the generation and display in 3-D of fractal shapes. For the first time, iteration with quaternions ($\mathbb{H}$) appeared. Subsequently, theoretical results have been treated for the quaternionic Mandelbrot set defined by the quadratic polynomial in the quaternions of the form q^2+c. However, S. Bedding and K. Briggs have established that there is "no interesting" dynamics for this approach and it does not play any fundamental role analogous to that for the map z^2+c in the complex plane.

- Recall: $\boxed{\mathbb{H}:=\{\, a + b\mathbf{i} + c\mathbf{j} + d\mathbf{k} : \mathbf{i}^2 = \mathbf{j}^2 = \mathbf{k}^2 = -1 \,\}}$

Quaternionic Dynamics

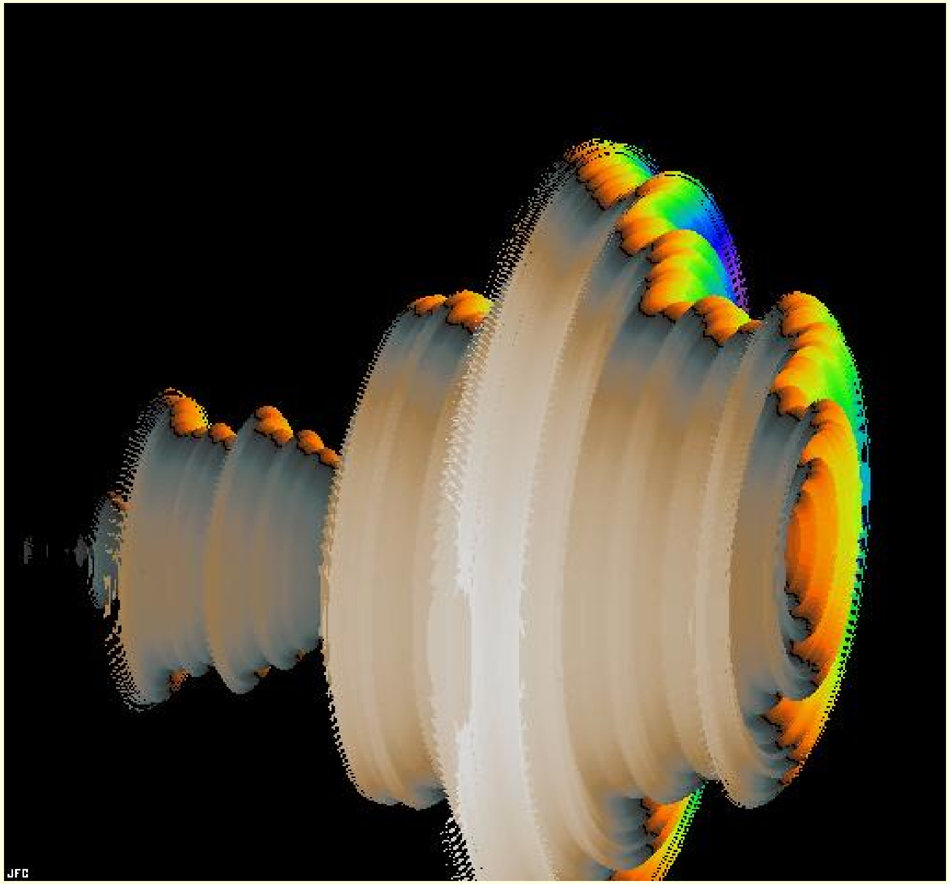

Author : Jean-François Colonna

Source : http://www.lactamme.polytechnique.fr

Author : Iñigo Quilez

Source : http://rgba.scenesp.org

Bicomplex Numbers

- In 1892, in search for a development of special algebras, Corrado Segre (1860-1924) published a paper in which he treated an infinite set of algebras whose elements he called bicomplex numbers, tricomplex numbers, …, n-complex numbers.
- We define **bicomplex numbers** as follows:

$$\mathbb{T} := \{\, a + b\mathbf{i_1} + c\mathbf{i_2} + d\mathbf{j} : \mathbf{i_1}^2 = \mathbf{i_2}^2 = -1,\ \mathbf{j}^2 = 1 \,\}$$

where $\boxed{\mathbf{i_2 j} = \mathbf{j i_2} = -\mathbf{i_1},\ \mathbf{i_1 j} = \mathbf{j i_1} = -\mathbf{i_2},\ \mathbf{i_2 i_1} = \mathbf{i_1 i_2} = \mathbf{j}}$

and $a, b, c, d \in \mathbb{R}$.

Bicomplex Numbers

- We remark that we can write a bicomplex number $a + b\mathbf{i_1} + c\mathbf{i_2} + d\mathbf{j}$ as

$$(a + b\mathbf{i_1}) + (c + d\mathbf{i_1})\,\mathbf{i_2} = z_1 + z_2\mathbf{i_2}$$

where $z_1, z_2 \in \mathbb{C}(\mathbf{i_1}) := \left\{\ x + y\mathbf{i_1} : \mathbf{i_1}^2 = -1 \right\}.$

The idempotent basis

- It is also important to know that every bicomplex number $z_1 + z_2\mathbf{i_2}$ has the following unique idempotent representation:

$$z_1 + z_2\mathbf{i_2} = (z_1 - z_2\mathbf{i_1})\mathbf{e_1} + (z_1 + z_2\mathbf{i_1})\mathbf{e_2}$$

where $\mathbf{e_1} = \dfrac{1+\mathbf{j}}{2}$ and $\mathbf{e_2} = \dfrac{1-\mathbf{j}}{2}$.

- This representation is very useful because: addition, multiplication and division can be done term-by-term. Also, an element will be non-invertible iff $z_1 - z_2\mathbf{i_1} = 0$ or $z_1 + z_2\mathbf{i_1} = 0$.

The idempotent basis

- From the idempotent basis, it is now possible to define the notion of the **bicomplex cartesian product**.

- **Definition 1**. *We say that* $X \subseteq \mathbb{T}$ *is a bicomplex cartesian set determined by* X_1 *and* X_2 *if*

$$X = X_1 \times_{\mathrm{e}} X_2 := \{\, z_1 + z_2\mathbf{i_2} \in \mathbb{T} : z_1 + z_2\mathbf{i_2} = w_1\mathbf{e_1} + w_2\mathbf{e_2},\ (w_1, w_2) \in X_1 \times X_2 \,\}.$$

Generalized Mandelbrot Set

Now, let us define a version of the Mandelbrot set for bicomplex numbers:

- **Definition 2**. *Let* $P_c(w) = w^2 + c$ *where* $w, c \in \mathbb{T}$ *and* $P_c^{\circ n}(w) := \left(P_c^{\circ(n-1)} \circ P_c\right)(w)$. *Then the generalized Mandelbrot set for bicomplex numbers is defined as follows:*

$$\mathcal{M}_2 = \left\{ c \in \mathbb{T} : P_c^{\circ n}(0) \not\to \infty \right\}.$$

From this definition we obtain the following result:

- **Theorem 1**. *The generalized Mandelbrot set* $\mathcal{M}_2$ *is connected.*

Generalized Filled-Julia Sets

It is also possible to generalized the notion of filled-Julia sets for the bicomplex numbers:

- **Definition 3**. *The generalized filled-Julia set for bicomplex numbers is defined as follows:*

$$\mathcal{K}_{2,c} = \left\{ w \in \mathbb{T} : P_c^{\circ n}(w) \not\to \infty \right\}$$

Finally, we obtain this relationship between the generalized Mandelbrot set and the generalized filled-Julia sets for the bicomplex numbers:

- **Theorem 2**. $c \in \mathcal{M}_2 \Leftrightarrow \mathcal{K}_{2,c}$ *is connected.*

Display in 3-D

- Previously, we established a version of the Mandelbrot set in dimension four. We are able now to give a version of the Mandelbrot set in dimension three using the definition for $\mathcal{M}_2$. The idea is to preserve the Mandelbrot set inside $\mathcal{M}_2$. Then, if we restrict the algorithm to the points of the form $a+b\mathbf{i_1}+c\mathbf{i_2}$ where $a, b, c \in \mathbb{R}$, we preserve the Mandelbrot set on two perpendicular complex planes and we stay in $\mathbb{R}^3$. This is the first argument to justify the following definition.

Dynamics of Several Complex Variables

- The polynomial $P_c(w) = w^2 + c$ is the following mapping of $\mathbb{C}^2$:

$$\left(z_1^2 - z_2^2 + c_1,\ 2z_1 z_2 + c_2\right).$$

where $w = z_1 + z_2\mathbf{i_2}$ and $c = c_1 + c_2\mathbf{i_2}$. We note that this mapping is not a **holomorphic automorphism** of $\mathbb{C}^2$.

The Tetrabrot

- **Definition 4**. *The "Tetrabrot" is defined as follows:*

$$\mathcal{T} = \left\{ a + b\mathbf{i_1} + c\mathbf{i_2} + d\mathbf{j} \in \mathbb{T} : d = 0 \text{ and } P_c^{\circ n}(0) \not\to \infty \right\}.$$

- It is possible to compute the infinite divergence layers of the Tetrabrot. We have to note at this step that each divergence layer will hide the others. For example, Fig. 2 is an illustration for the Tetrabrot of one of its divergence layers in correspondence with the divergence layer illustrated in Fig 1(A) for the Mandelbrot set.

The Tetrabrot

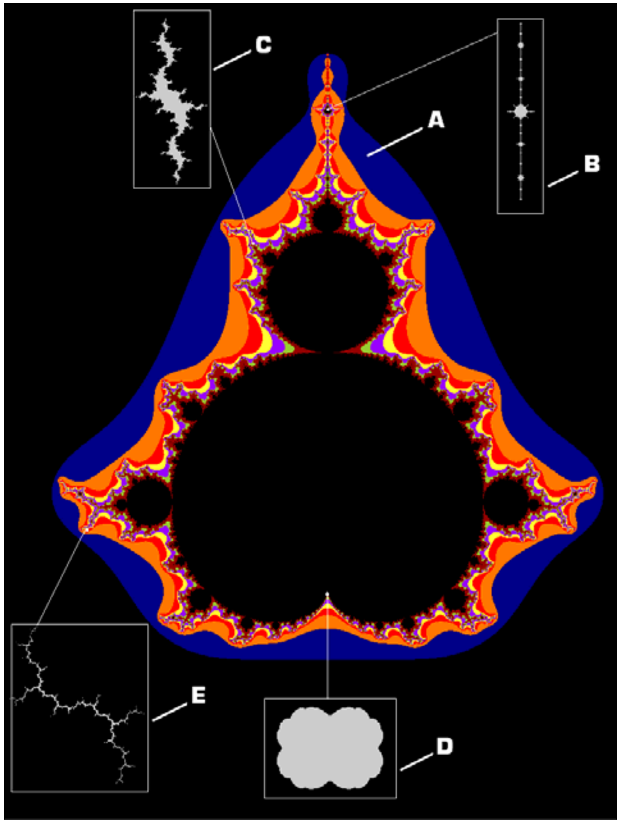

Fig. 1

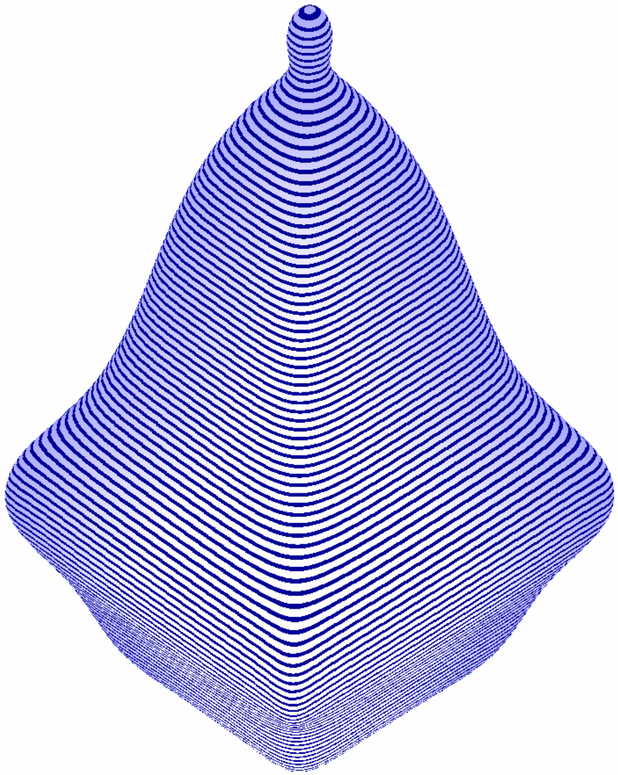

Fig. 2

The Tetrabrot

- In fact, the Tetrabrot is inside Fig. 2. It is possible to see a part of the Tetrabrot (see Fig. 3) if we cut a piece of Fig. 2.

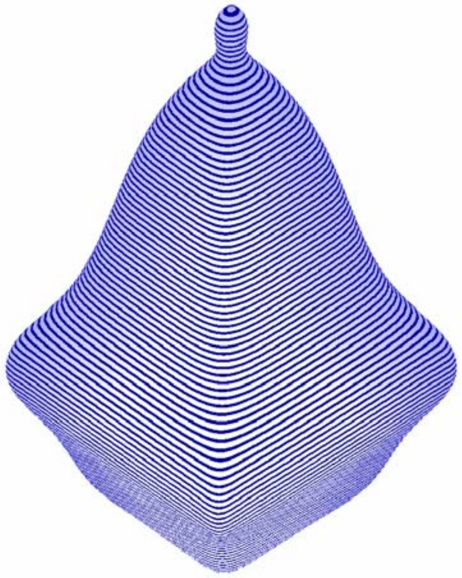

Fig. 2

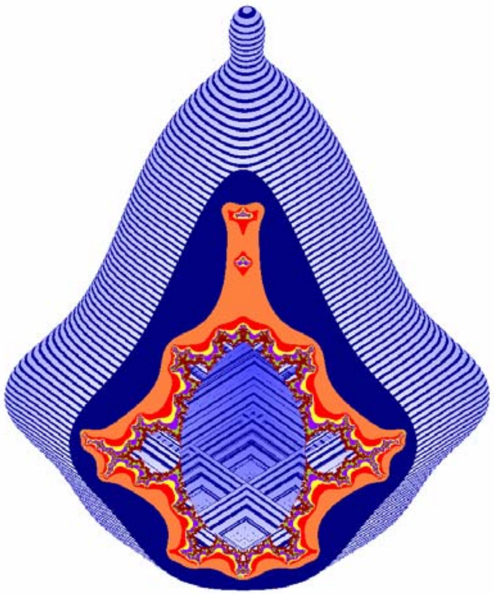

Fig. 3

The Tetrabrot

- In Fig 3, the colors represent the other divergence layers (see Figs 4, 5, 6 and 7). Figure 7 begins to be close to the set we wish to approach; then Fig 7 with its cut plane gives certainly a good idea of the Tetrabrot.

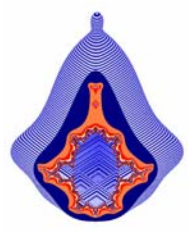

Fig. 3

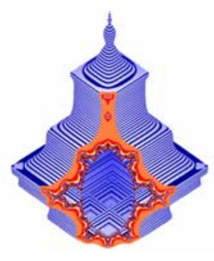

Fig. 4

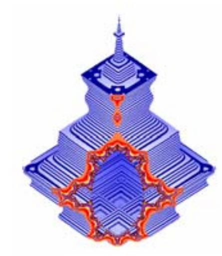

Fig. 5

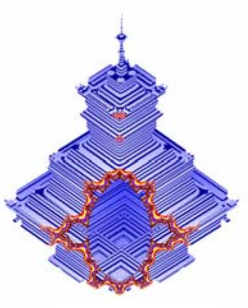

Fig. 6

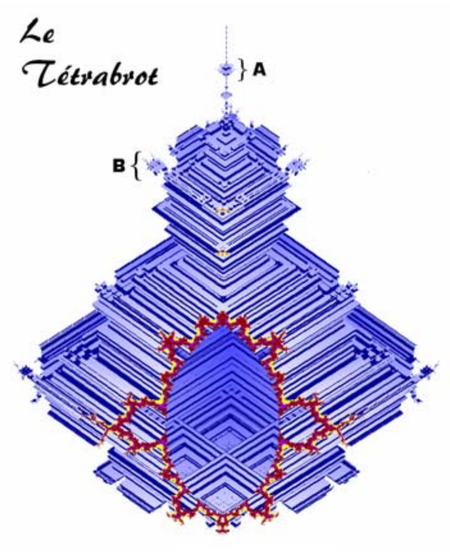

Fig. 7

The Tetrabrot

- Moreover, we observe that the specific enlargement of Fig. 7 between A and B (Fig. 8) confirms that the Tetrabrot could be disconnected.

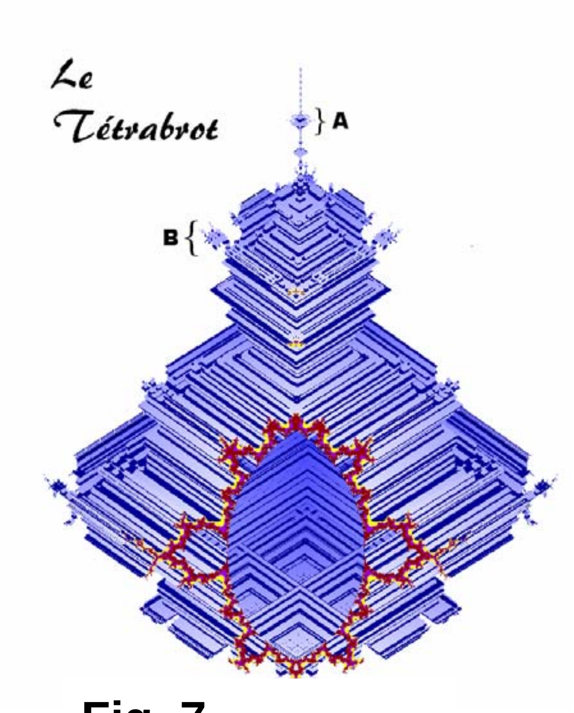

Fig. 7

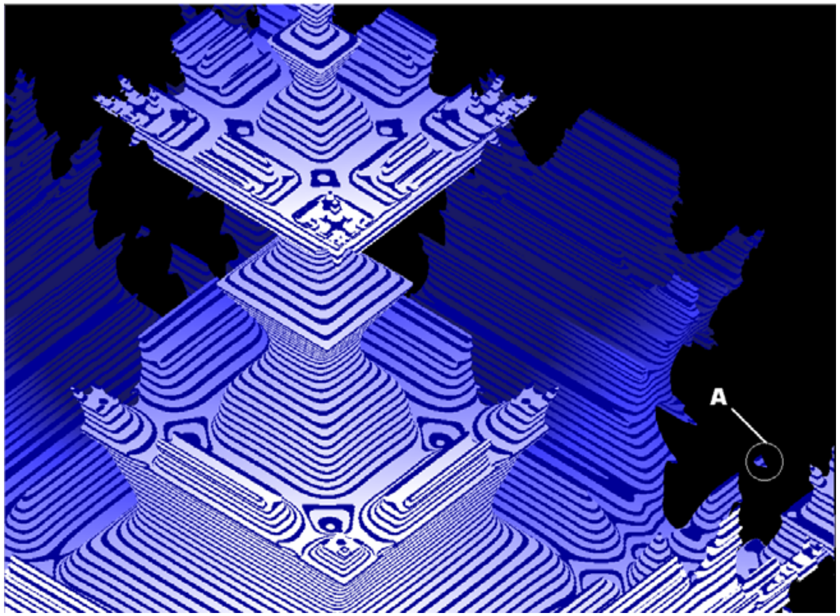

Fig. 8

The Tetrabrot

- Finally, to define the Tetrabrot we have put the last coordinate "**j**" equal to zero. In fact it is possible to do the same if we fix the last coordinate equal to a number different from zero. However, if we do that, we lose the beautiful symmetry of the Tetrabrot. Figure 9 gives an illustration of this phenomenon for a fixed "d**j**" with $d \neq 0$.

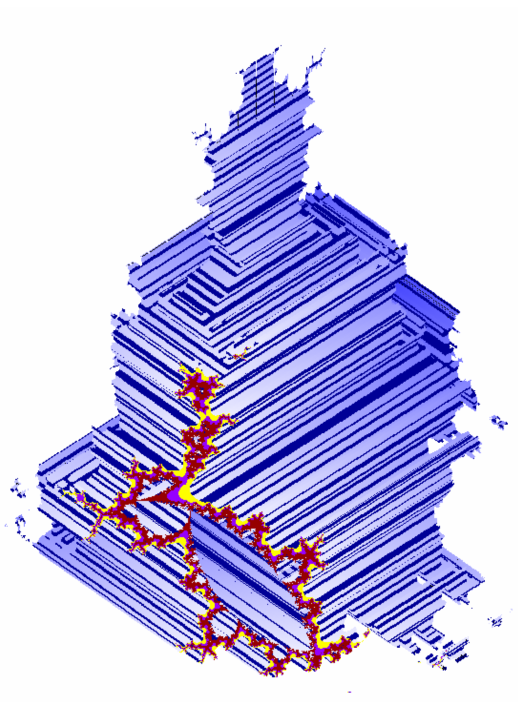

Fig. 9

The Cantor Set

- The following classical theorem establishes a connection between the Cantor sets and the filled-Julia sets:

- **Theorem 3 (P. Fatou and G. Julia)** *Let* $\mathcal{K}_c$ *be a filled-Julia set of the family of complex quadratic polynomials* $P_c(z) = z^2 + c$ *in the complex plane, and* $A_c\left(\infty\right) = \mathbb{C} / \mathcal{K}_c$ *the basin of attraction of for* $P_c(z) = z^2 + c$. *Then*

  (1) $0 \in \mathcal{K}_c \Leftrightarrow \mathcal{K}_c$ *is connected;*

  (2) $0 \in A_c \Leftrightarrow \mathcal{K}_c$ *is a Cantor set.*

The Cantor Set

Let us recall the definition of a Cantor set in $\mathbb{R}^n$:

- **Definition 5**. *A Cantor set is defined as a compact, perfect, totally disconnected subset in* $\mathbb{R}^n$.

- **Remark 1**. *Any such set is homeomorphic to the Cantor middle third set and therefore deserve the name of Cantor set.*

Basin of attraction of ∞

- Now, let us define the concept of basin of attraction of ∞ in the context of bicomplex numbers:

- **Definition 6**. *Let* $\mathcal{K}_{2,c}$ *be a filled-Julia set of the family of bicomplex quadratic polynomials* $P_c(w) = w^2 + c$ *in* $\mathbb{T}$. *We define* $\mathrm{A}_{2,c}(\infty) = \mathbb{T} \backslash \mathcal{K}_{2,c}$ *as the basin of attraction of* ∞ *for* $P_c(w) = w^2 + c$. *We note that*

$$A_{2,c}(\infty) = \left\{ w \in \mathbb{T} \,\middle|\, P_c^{\circ n}(w) \to \infty \right\}.$$

Generalized Fatou-Julia Theorem

- The next definition will be well justified in regard to the theorem below.
- **Definition 7**. *We define*

$$SA_{2,c}(\infty) = \left(\mathcal{K}_{c_1-c_2\mathbf{i_1}}\right)^c \times_e \left(\mathcal{K}_{c_1-c_2\mathbf{i_1}}\right)^c$$
$$= A_{c_1-c_2\mathbf{i_1}}(\infty) \times_e A_{c_1+c_2\mathbf{i_1}}(\infty)$$

as the strong basin of attraction of ∞ for $P_c(w) = w^2 + c$ where $c = (c_1 - c_2\mathbf{i_1})\mathbf{e_1} + (c_1 + c_2\mathbf{i_1})\mathbf{e_2}$.

We note that:

$$SA_{2,c}(\infty) \subset A_{2,c}(\infty).$$

Generalized Fatou-Julia Theorem

- The following theorem gives a characterization of the filled-Julia sets for bicomplex numbers and introduces naturally the idea of Cantor sets in $\mathbb{R}^4$.
- **Theorem 4 (Fatou-Julia Theorem in $\mathbb{T}$)** *Let $\mathcal{K}_{2,c}$ be a filled-Julia set for bicomplex numbers and $c \in \mathbb{T}$. Then*

(1) $0 \in \mathcal{K}_{2,c} \Leftrightarrow \mathcal{K}_{2,c}$ *is connected;*

(2) $0 \in SA_{2,c}(\infty) \Leftrightarrow \mathcal{K}_{2,c}$ *is a Cantor set in $\mathbb{T}$;*

(3) $0 \in A_{2,c}(\infty) \setminus SA_{2,c}(\infty) \Leftrightarrow \mathcal{K}_{2,c}$ *is disconnected but not totally disconnected.*

Generalized Fatou-Julia Theorem

- Now it is possible to illustrate by figures in $\mathbb{R}^3$ the connections between the various cases of the last theorem when the filled-Julia sets come from points around or inside the Tetrabrot. In fact, we are in the case 1 of the last theorem if and only if the filled-Julia sets come from points inside the Tetrabrot. The other cases are established from points inside the infinite divergence layers of the Tetrabrot. Fig 10 and 11 are an illustration of this phenomenon where the red zones are the points c which satisfy the case 3 and the other colors the points c which satify the case 2.

Generalized Fatou-Julia Theorem

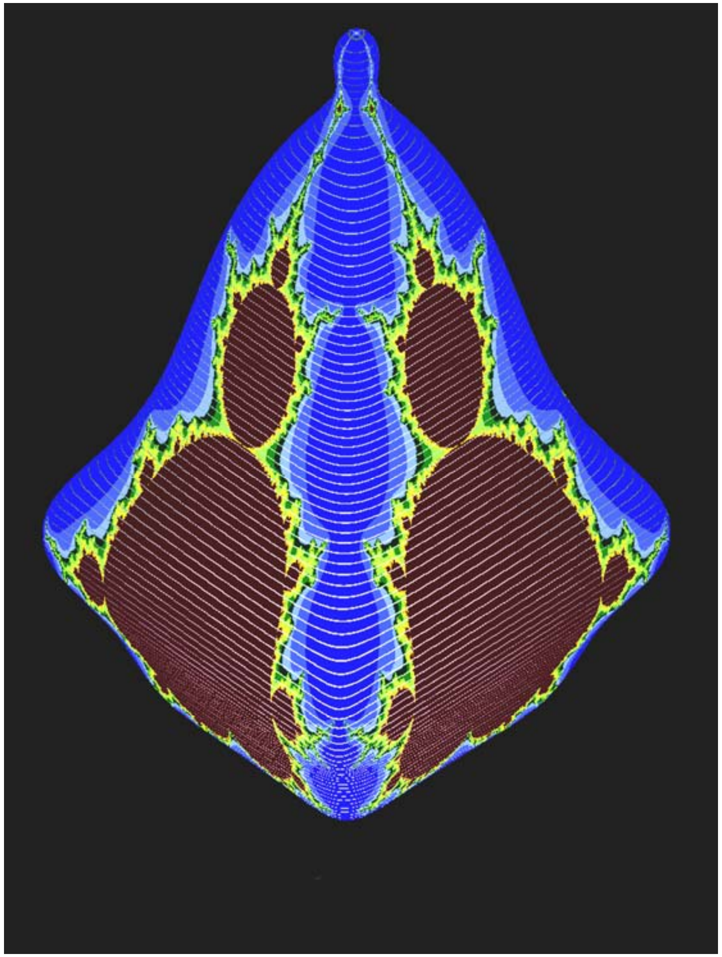

Fig. 10

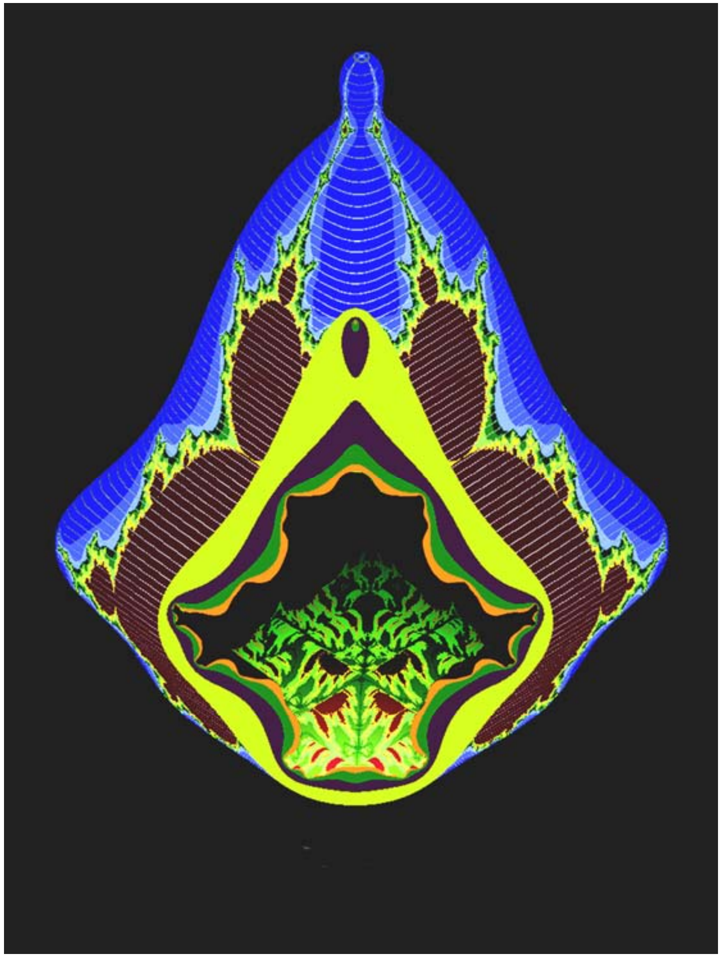

Fig. 11

Generalized Fatou-Julia Theorem

- More specifically, the Fig. 11 makes it possible to observe this phenomenon on the bottom inside the Tetrabrot for a specific divergence layer; the colors on the cut plane are an illustration of the other divergence layers of the Tetrabrot. We note also that the colors for the case 2 have been computed from the average of each divergence layer obtained from the number of iterations needed to know that zero is inside $A_{c_1 - c_2 \mathbf{i_1}}(\infty)$ and $A_{c_1 + c_2 \mathbf{i_1}}(\infty)$.

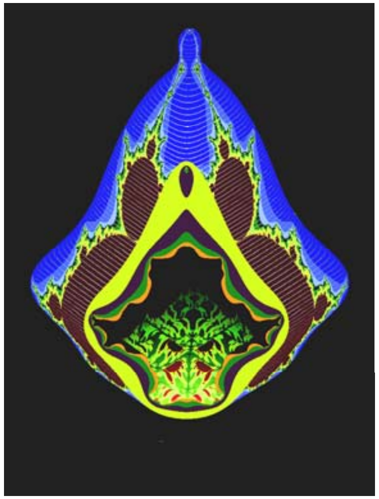

Fig. 11

The filled-Julia sets in $\mathbb{R}^3$

- The same process as for the Tetrabrot yields a version of the filled-Julia sets in $\mathbb{R}^3$. The next definition defined the bicomplex filled-Julia sets in $\mathbb{R}^3$.
- **Definition 8**. *A bicomplex filled-Julia set in* $\mathbb{R}^3$ *is defined as follows:* ($c \in \mathbb{T}$)

$$\mathcal{L}_{2,c} = \left\{ w = a + b\mathbf{i_1} + c\mathbf{i_2} + d\mathbf{j} \in \mathrm{T} \colon d = 0 \text{ and } P_c^{\circ n}\left(w\right) \not\to \infty \right\}.$$

The filled-Julia sets in $\mathbb{R}^3$

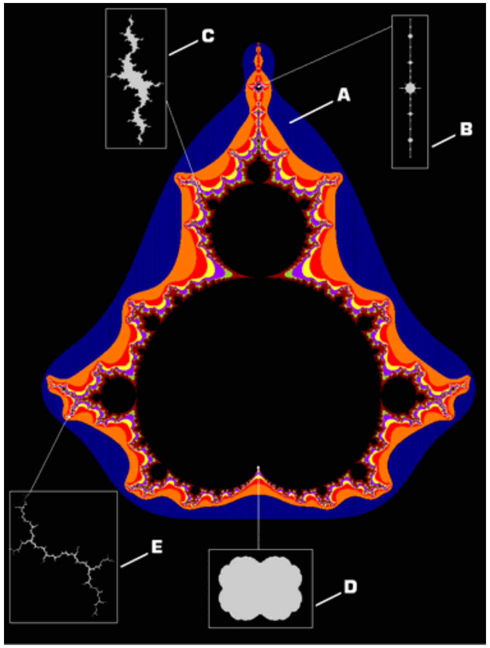

Fig. 1

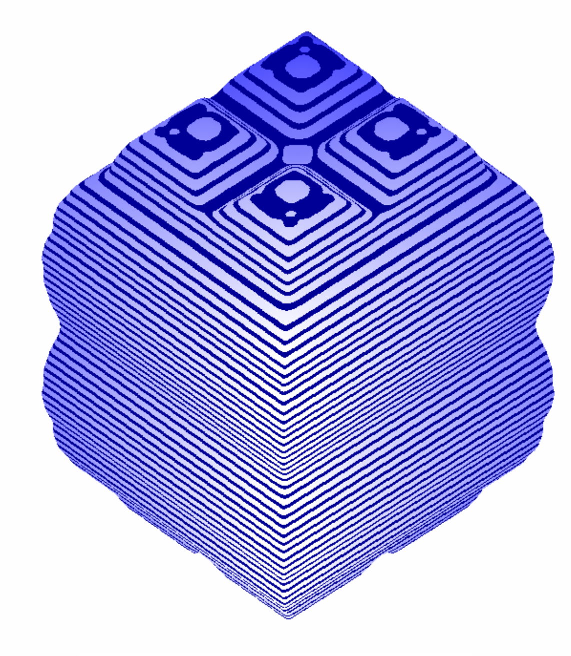

Fig. 12

- Figure 12 is an illustration of the filled-Julia set for the Tetrabrot at the same point c = 0.25 as the filled-Julia set D of Fig. 1. Hence, Fig. 12 is a kind of generalization of the filled-Julia set $K_{0.25}$ in the complex plane.

The filled-Julia sets in $\mathbb{R}^3$

- In the same manner, Figs. 13-16 are an illustration of the filled-Julia set at $c = \mathbf{i_1}$ for different divergence layers to infinity. We remark that Fig. 16 is a good approximation of this set and an interesting generalizationof Fig. 1(E).

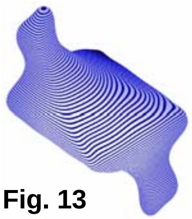

Fig. 13

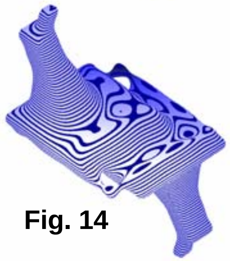

Fig. 14

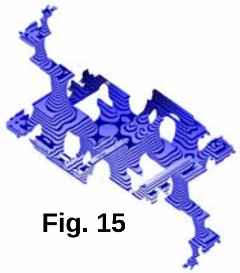

Fig. 15

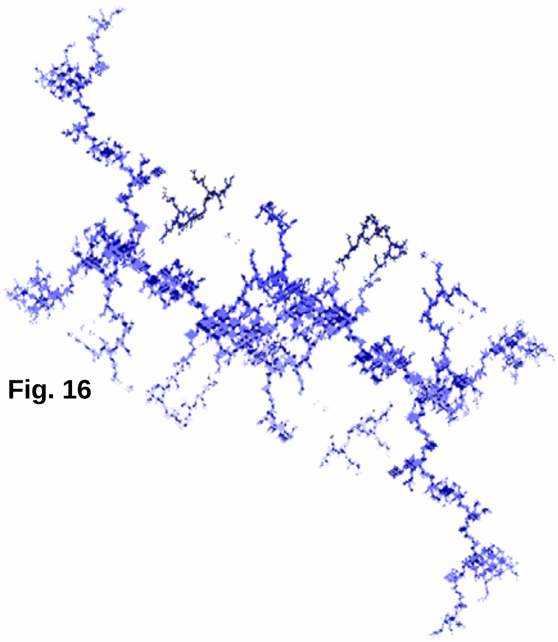

Fig. 16

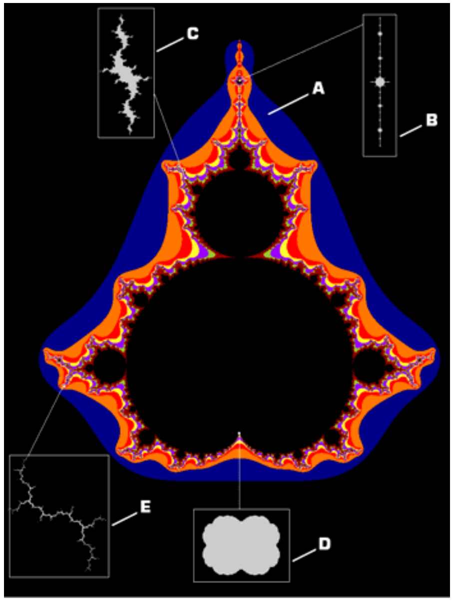

Fig. 1

“Cantor sets” in $\mathbb{R}^3$

The same process can also be used when the filled-Julia sets are not connected. In that case we established these following results:

- **Lemma 1**. *Let* $c \in \mathbb{T}$ *and* $\mathcal{K}_{2,c}$ *a Cantor set in* $\mathbb{R}^4$ *Then* $\mathcal{L}_{2,c}$ *is compact and totally disconnected in* $\mathbb{R}^3$.
- **Theorem 5**. *Let* $c \in \mathbb{C}(\mathbf{i_1}) := \left\{ x + y\mathbf{i} : \mathbf{i_1}^2 = -1 \right\}$ *and* $\mathcal{K}_c$ *a Cantor set. Then,* $\mathcal{K}_{2,c}$ *is a Cantor set in* $\mathbb{R}^4$ *and* $\mathcal{L}_{c,2}$ *is the union of a Cantor set in* $\mathbb{R}^3$ *and a set which is* ***at most countable****.*

"Cantor sets" in $\mathbb{R}^3$

- Figures 17-34 give an illustration of such "Cantor sets" in $\mathbb{R}^3$. In fact, Figs. 17-22 and 23-29 are respectively close to the filled-Julia sets of Fig. 12 and 13 without coming from points inside the Tetrabrot.

Fig. 17

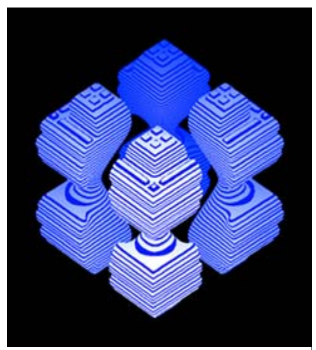

Fig. 18

Fig. 19

Fig. 20

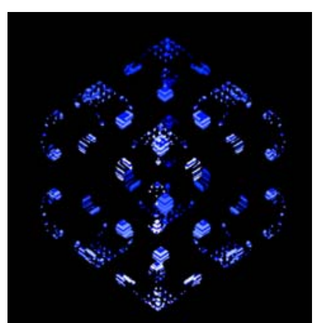

Fig. 21

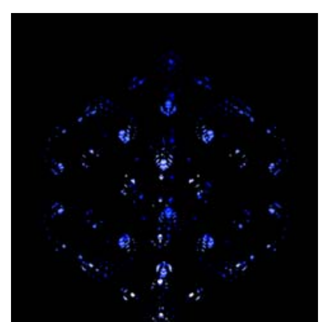

Fig. 22

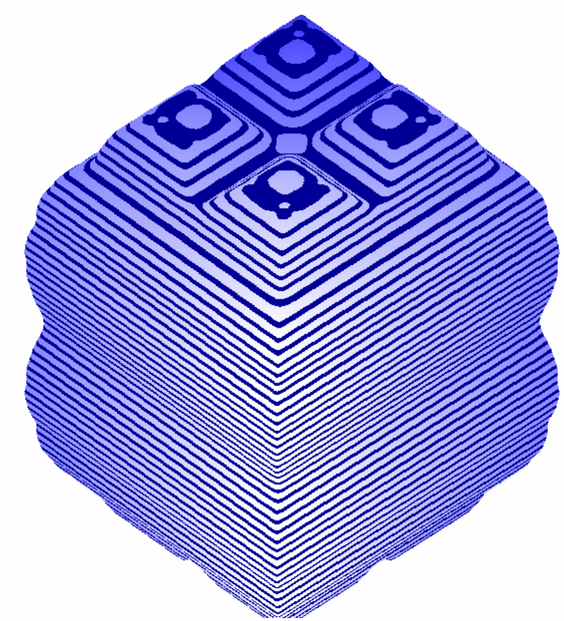

Fig. 12

“Cantor sets” in $\mathbb{R}^3$

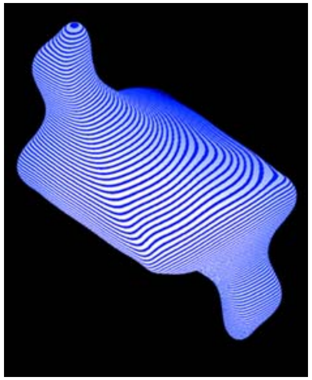
Fig. 18

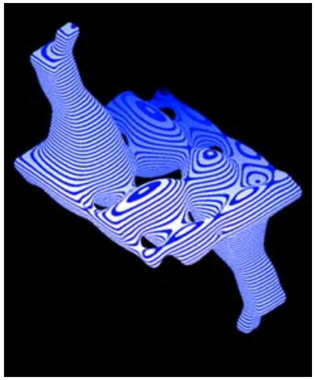
Fig. 19


Fig. 20

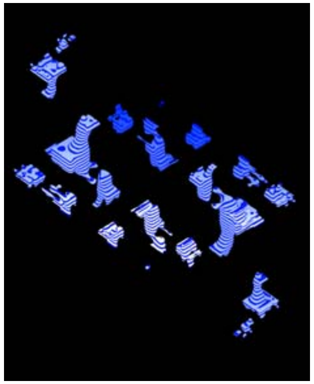
Fig. 21

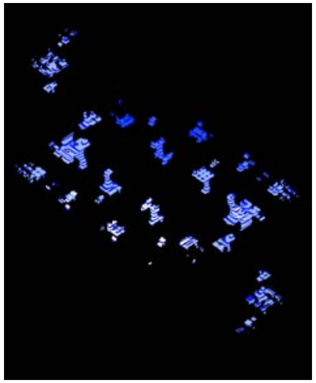
Fig. 22

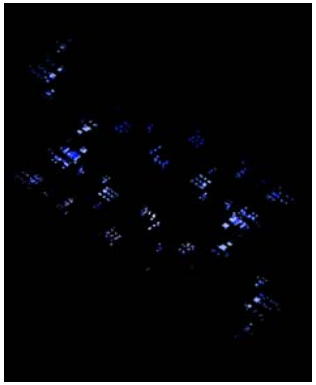
Fig. 23

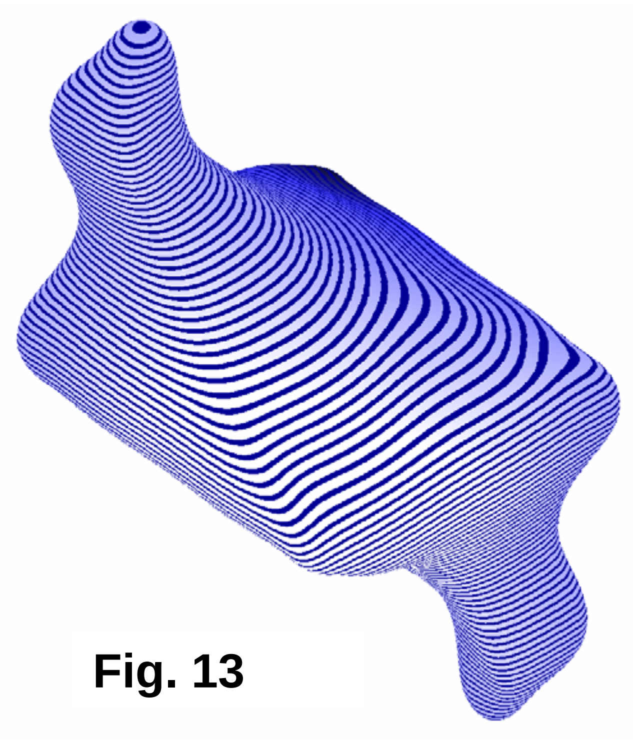
Fig. 13

- In each case, each step used a divergence layer to infinity closer to the true set. With this construction, we remark that we visually obtain a result similar to the geometric construction of the Cantor middle third set.

“Cantor sets” in $\mathbb{R}^3$

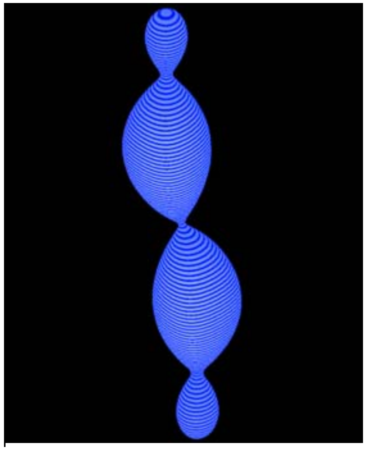

Fig. 24

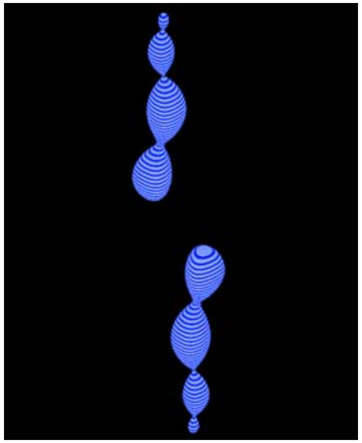

Fig. 25

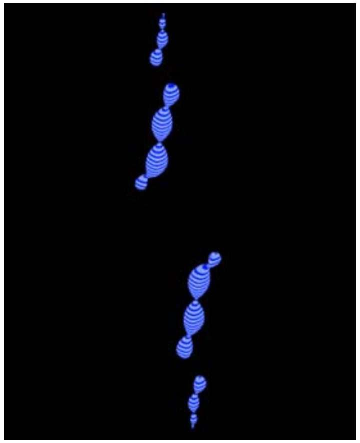

Fig. 26

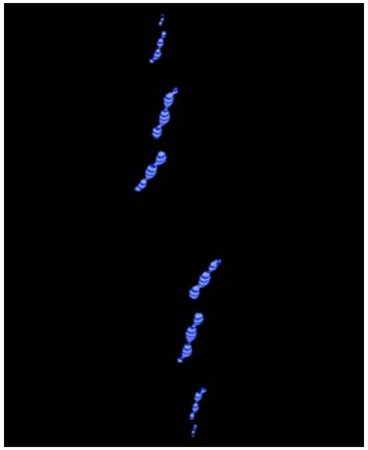

Fig. 27

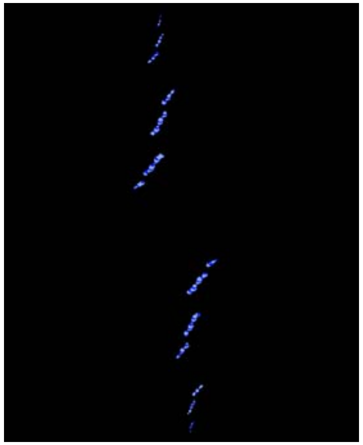

Fig. 28

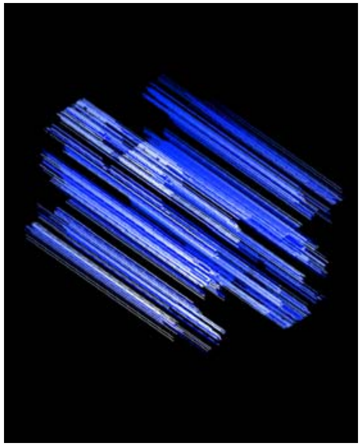

Fig. 29

- Morever, Fig. 29 is an ilustration of $\mathcal{L}_{2,c}$ for a filled-Julia set $\mathcal{K}_{2,c}$ where:

  $$0 \in A_{2,c}(\infty) \setminus SA_{2,c}(\infty).$$

- We note that this set in $\mathbb{R}^3$ has connected components.

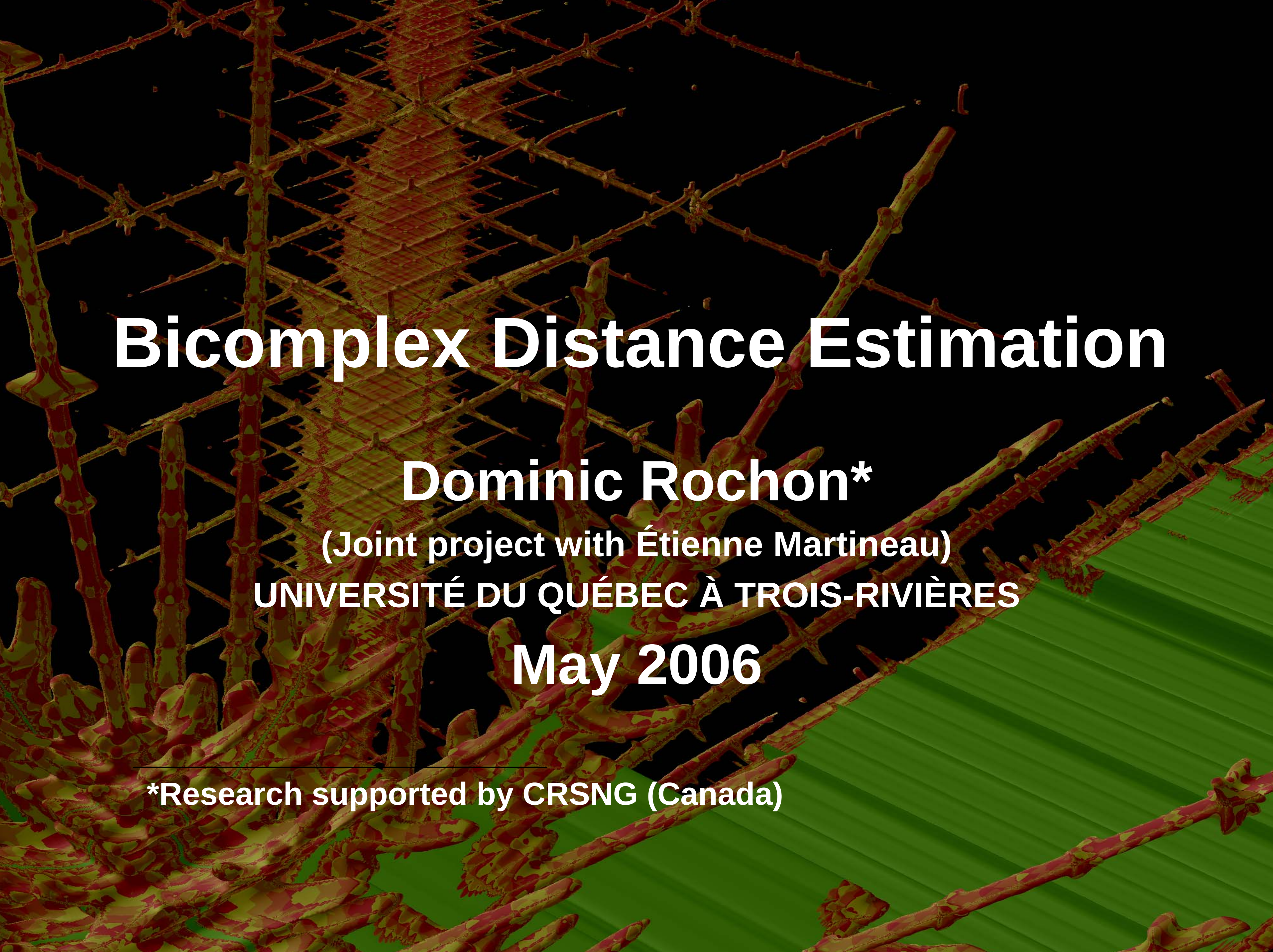

Bicomplex Distance Estimation

Dominic Rochon*

(Joint project with Étienne Martineau)

UNIVERSITÉ DU QUÉBEC À TROIS-RIVIÈRES

May 2006

***Research supported by CRSNG (Canada)**

Outline : Bicomplex Distance Estimation

- Bicomplex Numbers
- Bicomplex Distance Estimation for the Tetrabrot
  - Distance Formulas
  - Approximated Distance Formulas
- Applications
  - Ray-tracing
  - Exploration

Bicomplex Numbers

- The norm used on $\mathbb{T}$ is the Euclidean norm (noted $|\ |$) of $\mathbb{R}^4$ and the following formula is true over the set of bicomplex numbers:

$$\left|z_1 + z_2\mathbf{i_2}\right| = \left(\frac{\left|z_1 - z_2\mathbf{i_1}\right|^2 + \left|z_1 + z_2\mathbf{i_1}\right|^2}{2}\right)^{1/2}.$$

Bicomplex Numbers

- The set

$$\mathbb{D} := \{x + y\mathbf{j} \mid x, y \in \mathbb{R}\}$$

will be called the set of hyperbolic numbers (also called duplex numbers) and

$$|w|_{\mathbf{j}} := |z_1 - z_2\mathbf{i_1}|\mathbf{e_1} + |z_1 + z_2\mathbf{i_1}|\mathbf{e_2} \in \mathbb{D}.$$

- Will be referred to as the modulus in **j** of $w = z_1 + z_2\mathbf{i_2}$.

Bicomplex Numbers

- This specific modulus satisfies the following properties:

(1) $\big||w|_{\mathbf{j}}\big| = |w| = \sqrt{\mathrm{Re}\left(|w|_{\mathbf{j}}^{2}\right)}$;

(2) $|w|_{\mathbf{j}} = 0$ if and only if $w = 0$;

(3) $|w_1 \cdot w_2|_{\mathbf{j}} = |w_1|_{\mathbf{j}}\,|w_2|_{\mathbf{j}} \quad \forall w_1, w_2 \in \mathbb{T}.$

Distance Estimation for the Tetrabrot

- Let us begin with the following well known result about the distance estimation for the filled-Julia sets in the complex plane.
- **Theorem 1**. *Let* $d(z, K_b) = \inf\{|z - a| : a \in \mathcal{K}_b\}$ *be defined as the distance from* $z \in \mathbb{C}$ *to the filled-Julia set* $\mathcal{K}_b$ *with* $b \in \mathcal{M}$. *Then the distance* $d(z_0, \mathcal{K}_b)$ *between* z_0 *lying outside of* $\mathcal{K}_b$ *and* $\mathcal{K}_b$ *itself satisfies*

$$\frac{\sinh\left[G(z_0)\right]}{2e^{G(z_0)}\left|G'(z_0)\right|} < d(z_0, \mathcal{K}_b) < \frac{2\sinh\left[G(z_0)\right]}{\left|G'(z_0)\right|}.$$

Where $G(z_0)$ *is the potential at the point* z_0.

Distance Estimation for the Tetrabrot

- We will express the distance form a point $w \in \mathbb{T}$ to a bicomplex filled-Julia set in terms of two distances in the complex plane (in $\mathbf{i_1}$).
- **Lemma 1**. *Let* $d(w, \mathcal{K}_{2,c}) = \inf\{|w - a| : a \in \mathcal{K}_{2,c}\}$ *be defined as the "bicomplex" distance from* $w = z_1 + z_2\mathbf{i_2} \in \mathbb{T}$ *to the bicomplex filled-Julia set* $\mathcal{K}_{2,c}$ *where* $c = c_1 + c_2\mathbf{i_2} \in \mathbb{T}$. *Hence,* $d(w, \mathcal{K}_{2,c}) =$

$$\left[\frac{\left[d\left(z_1 - z_2\mathbf{i_1}, \mathcal{K}_{c_1 - c_2\mathbf{i_1}}\right)\right]^2 + \left[d\left(z_1 + z_2\mathbf{i_1}, \mathcal{K}_{c_1 + c_2\mathbf{i_1}}\right)\right]^2}{2}\right]^{1/2}.$$

Distance estimation for the Tetrabrot

- **Definition 1**. *Let* $G_1(z_1 - z_2\mathbf{i_1})$ *and* $G_2(z_1 + z_2\mathbf{i_1})$ *be two electrostatic potentials. The bicomplex potential, at a point* $w = z_1 + z_2\mathbf{i_2} \in \left(\mathbb{C}(\mathbf{i_1}) \setminus \mathcal{K}_{b_1}\right) \times_e \left(\mathbb{C}(\mathbf{i_1}) \setminus \mathcal{K}_{b_2}\right)$ *is defined as*

$$G(w) := G_1(z_1 - z_2\mathbf{i_1})\mathbf{e_1} + G_2(z_1 + z_2\mathbf{i_1})\mathbf{e_2} \in \mathbb{D}$$

and

$$G'(w) := G_1'(z_1 - z_2\mathbf{i_1})\mathbf{e_1} + G_2'(z_1 + z_2\mathbf{i_1})\mathbf{e_2} \in \mathbb{D}.$$

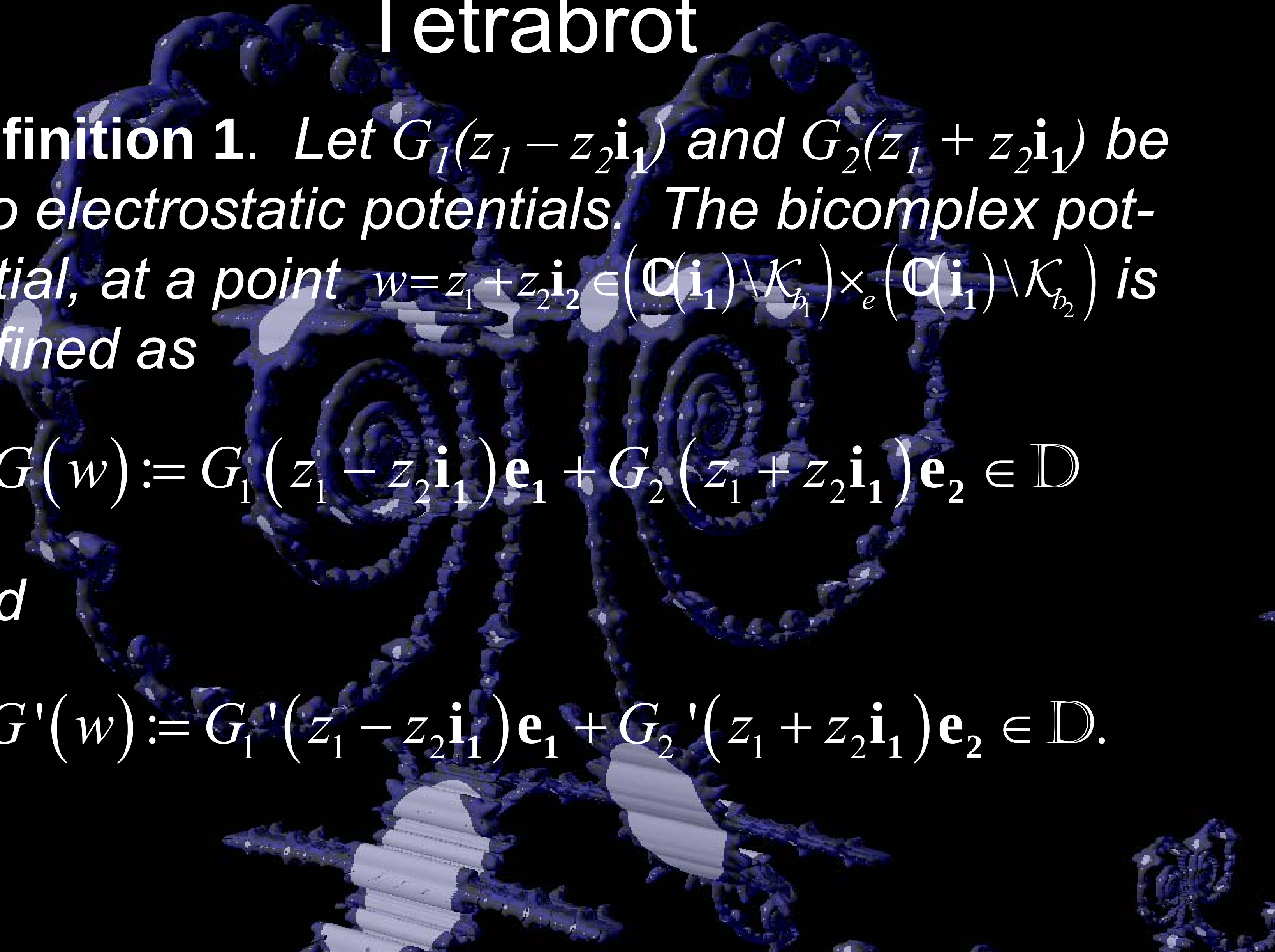

Distance estimation for the Tetrabrot

- In $\mathbb{T}$, the bicomplex logarithm $\ln(z_1 + z_2\mathbf{i_1})$ is defined to be the inverse of the bicomplex exponential function:

$$e^{z_1+z_2\mathbf{i_2}} := e^{z_1}\left[\cos(z_2)+\mathbf{i_2}\sin(z_2)\right].$$

With this definition of the bicomplex logarithm, it is possible to express the bicomplex potential in a similar way to that used for one complex variable. Let $\mathbb{T}\backslash_e \mathcal{K}_{2,c} := \left(\mathbb{C}(\mathbf{i_1})\backslash\mathcal{K}_{c_1-c_2\mathbf{i_1}}\right)\times_e\left(\mathbb{C}(\mathbf{i_1})\backslash\mathcal{K}_{c_1+c_2\mathbf{i_1}}\right)$.

- **Theorem 2**. *Let* $G:\mathbb{T}\backslash_e \mathcal{K}_{2,c}\to D$ *be a bicomplex potential and* $c=(c_1-c_2\mathbf{i_1})\mathbf{e_1}+(c_1+c_2\mathbf{i_1})\mathbf{e_2}$. *Then*

- $$G(w)=\ln\left|\phi_c(w)\right|_j \quad \forall w\in\mathbb{T}$$
-

where $\phi_c:\mathbb{T}\backslash_e \mathcal{K}_{2,c}\to\mathbb{T}\backslash_e \overline{B^1(0,1)}\times_e\overline{B^1(0,1)}$ *is biholomorphic in terms of two complex variables.*

Distance Formulas

- We are now ready to state the major result of this talk.
- **Theorem 3**. *Let* $w_0 = z_1 + z_2\mathbf{i_1} \in \mathbb{T}$ *and* $c_1 + c_2\mathbf{i_2} \in \mathcal{M}_2$. *Then the distance* $d(w_0, \mathcal{K}_{2,c})$ *between* w_0 *lying outside of* $\mathcal{K}_{2,c}$ *and* $\mathcal{K}_{2,c}$ *itself satisfies:*

(1) If $w_0 \in \mathbb{T}\backslash_e \mathcal{K}_{2,c}$,

$$\left|\frac{\sinh\left[G\left(w_0\right)\right]}{2e^{G(w_0)}G'\left(w_0\right)}\right| < d\left(w_0, \mathcal{K}_{2,c}\right) < \left|\frac{2\sinh\left[G\left(w_0\right)\right]}{G'\left(w_0\right)}\right|$$

where $G(w_0)$ *is the bicomplex potential at the point* w_0.

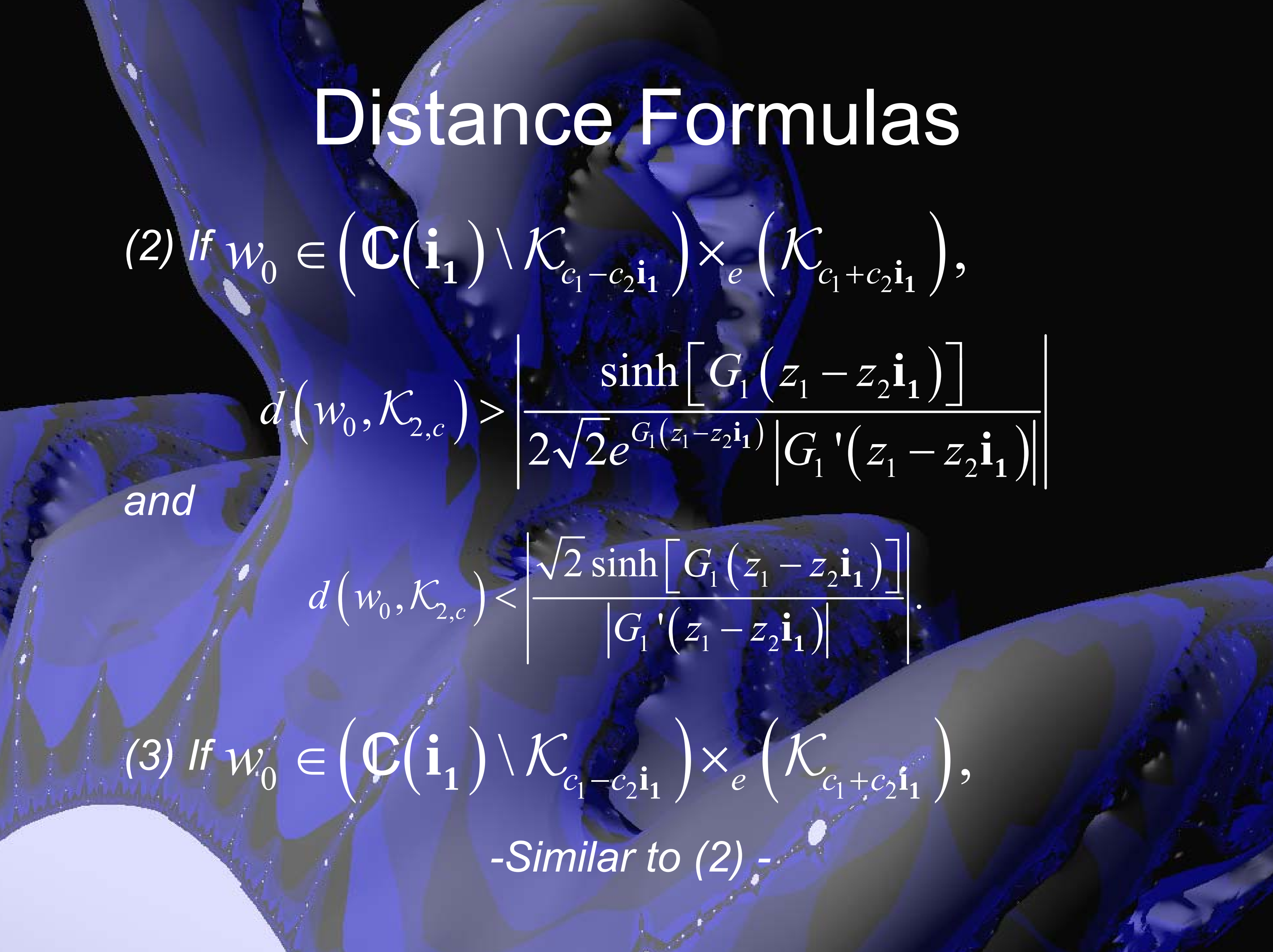

Distance Formulas

(2) If $w_0 \in \left(\mathbb{C}(\mathbf{i_1}) \setminus \mathcal{K}_{c_1 - c_2\mathbf{i_1}}\right) \times_e \left(\mathcal{K}_{c_1 + c_2\mathbf{i_1}}\right)$,

$$d\left(w_0, \mathcal{K}_{2,c}\right) > \left| \frac{\sinh\left[G_1\left(z_1 - z_2\mathbf{i_1}\right)\right]}{2\sqrt{2}e^{G_1\left(z_1 - z_2\mathbf{i_1}\right)}\left|G_1'\left(z_1 - z_2\mathbf{i_1}\right)\right|} \right|$$

and

$$d\left(w_0, \mathcal{K}_{2,c}\right) < \left| \frac{\sqrt{2}\sinh\left[G_1\left(z_1 - z_2\mathbf{i_1}\right)\right]}{\left|G_1'\left(z_1 - z_2\mathbf{i_1}\right)\right|} \right|.$$

(3) If $w_0 \in \left(\mathbb{C}(\mathbf{i_1}) \setminus \mathcal{K}_{c_1 - c_2\mathbf{i_1}}\right) \times_e \left(\mathcal{K}_{c_1 + c_2\mathbf{i_1}}\right)$,

-Similar to (2) -

Approximated Distance Formulas

- **Theorem 4.** *Let* $w_0 = z_1 + z_2\mathbf{i_2} \in \mathcal{M}_2$. *Then, the distance* $d(w_0, \mathcal{K}_{2,c})$ *between* w_0 *lying outside of* $\mathcal{K}_{2,c}$ *and* $\mathcal{K}_{2,c}$ *itself approximatly satisfies:*
  (1) If $w_0 \in \mathbb{T} \setminus_e \mathcal{K}_{2,c}$,

$$\left|\frac{w_n \ln|w_n|_j}{2|w|_j^{\frac{1}{2^n}} w_n'}\right| < d\left(w_0, \mathcal{K}_{2,c}\right) < \left|2\frac{w_n}{w_n'}\ln|w_n|_j\right|$$

where $w_n := P_c^{\circ n}\left(w_0\right)$

and $w_n' := \dfrac{d}{dw}\left[P_c^{\circ n}\left(w\right)\right]\Big|_{w=w_0} \quad \forall n \in \mathbb{N}.$

Approximated Distance Formulas

(2) If $w_0 \in \left(\mathbb{C}(\mathbf{i_1}) \setminus \mathcal{K}_{c_1 - c_2\mathbf{i_1}}\right) \times_e \left(\mathcal{K}_{c_1 + c_2\mathbf{i_1}}\right),$

$$d\left(w_0, \mathcal{K}_{2,c}\right) > \left| \frac{\left|z_{1,n} - z_{2,n}\mathbf{i_1}\right| \ln\left|z_{1,n} - z_{2,n}\mathbf{i_1}\right|}{2\sqrt{2}\left|z_{1,n} - z_{2,n}\mathbf{i_1}\right|^{\frac{1}{2^n}} \left(z_{1,n} - z_{2,n}\mathbf{i_1}\right)'} \right|$$

$$d\left(w_0, \mathcal{K}_{2,c}\right) < \frac{\sqrt{2}\left|z_{1,n} - z_{2,n}\mathbf{i_1}\right|}{\left|\left(z_{1,n} - z_{2,n}\mathbf{i_1}\right)_n'\right|} \ln\left|z_{1,n} - z_{2,n}\mathbf{i_1}\right|$$

where $z_{1,n} - z_{2,n}\mathbf{i_1} := P_c^{\circ n}\left(z_1 - z_2\mathbf{i_1}\right)$

and $\left(z_{1,n} - z_{2,n}\mathbf{i_1}\right)' := \frac{d}{dz}\left[P_c^{\circ n}(z)\right]\Big|_{z = z_{1,n} - z_{2,n}\mathbf{i_1}}.$

Approximated Distance Formulas

(3) If $w_0 \in \left(\mathbb{C}(\mathbf{i_1}) \setminus \mathcal{K}_{c_1 - c_2\mathbf{i_1}}\right) \times_e \left(\mathcal{K}_{c_1 + c_2\mathbf{i_1}}\right),$

- similar to (2) -

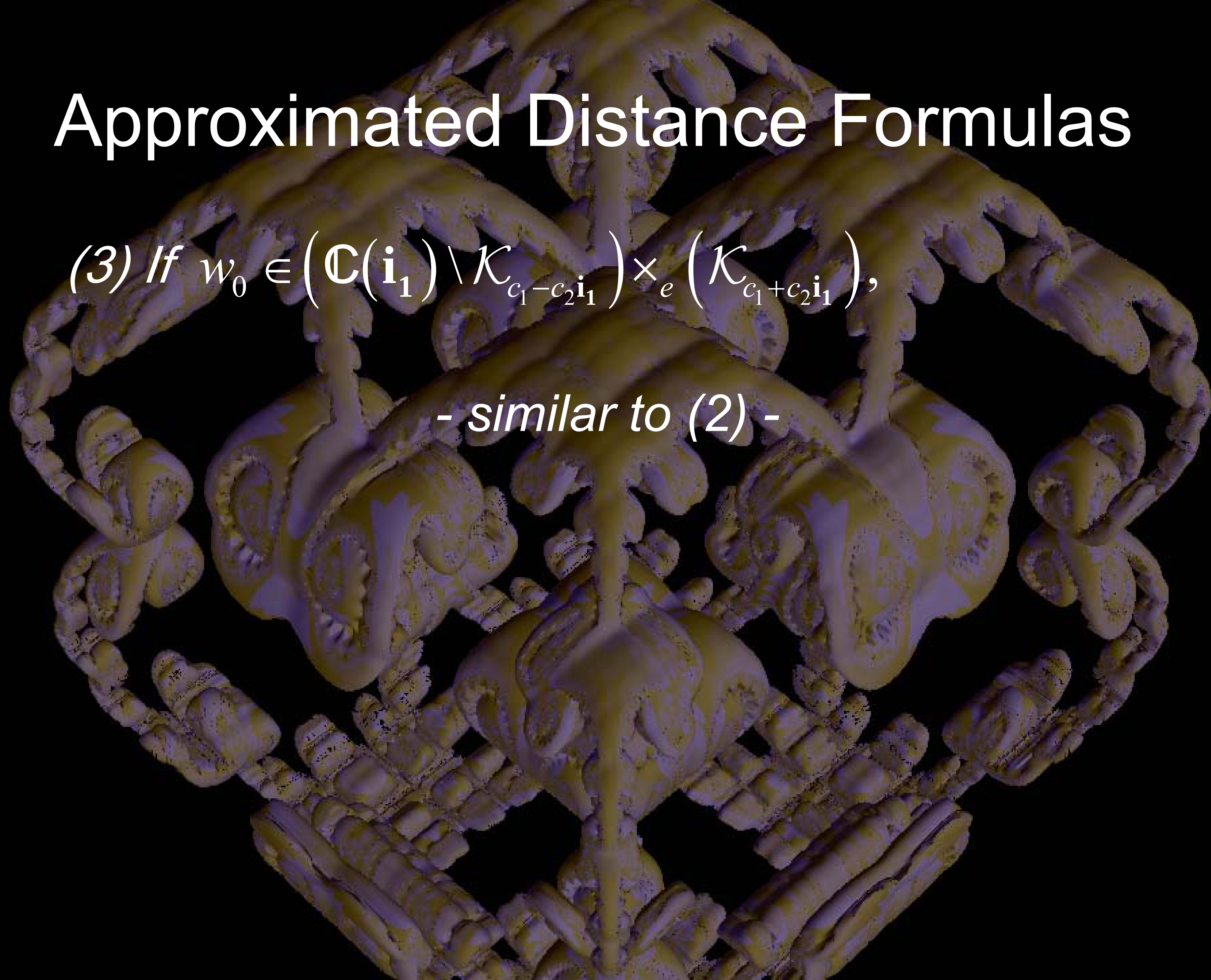

Ray-Tracing

- Now we use the lower bound distance estimation formula D_l in conjunction with ray-tracing to produce images of bicomplex fractals.
- Let $\vec{v}$ be an unitary vector in $\mathbb{R}^4$ and μ a point in $\mathbb{T} \backslash \mathcal{K}_{2,c}$. Now define

$$\left\{Z_{\mu,\vec{v},n}\right\} := \begin{cases} Z_{\mu,\vec{v},0} = \mu \\ Z_{\mu,\vec{v},n} = Z_{\mu,\vec{v},n-1} + D_l\left(Z_{\mu,\vec{v},n-1}\right)\vec{v}. \end{cases}$$

- By definition, no point in $\mathcal{K}_{2,c}$ can be a member of such sequence.

Ray-Tracing

- If we set the projection eye to μ and use $\vec{v}$ as the orientation of our ray, then

$$\lim_{n\to\infty} Z_{\mu,\vec{v},n}$$

is our ray-tracing algorithm.

- Two things may happen, we may miss the fractal or we may converge i.e.

$$\sum_{n=0}^{\infty} D_l\left(Z_{\mu,\vec{v},n}\right) = \infty$$

or

$$\sum_{n=0}^{\infty} D_l\left(Z_{\mu,\vec{v},n}\right) < \infty \Rightarrow \lim_{n\to\infty} D_l\left(Z_{\mu,\vec{v},n}\right) = 0.$$

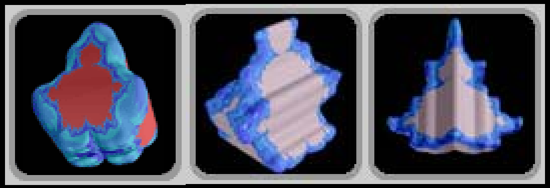

Exploration

- The images of the fractals will be drawn on a screen, noted S that is defined by four coplanar points in space. These points are our screen corner. We divide S into pixel according to the resolution desired for our image. The position of the eye μ, will be function of the position and size of S. When we move S, μ will follow. We compute the first image of the object and while tracing the fractal, we keep stored the distance of the object.

Exploration

- To zoom into the region of interest, few steps are necessary. First we must recenter the selected region by rotation from μ, then resize the screen to the region of interest. Next, using a fraction of distance to the object, we move S forward. A typical implementation could use the ratio screen size region of interest of the fractal distance. As we get closer to the fractal, we should lower the ε value to keep a good level of fractal details.

More details available on my web site:

www.3dfractals.com

Dominic Rochon

Département de mathématiques et d’informatique

Université du Québec à Trois-Rivières

C.P. 500 Trois-Rivières, Québec

Canada, G9A 5H7

E-mail: Dominic.Rochon@uqtr.ca

Tetrabrot inside the Tetrabrot

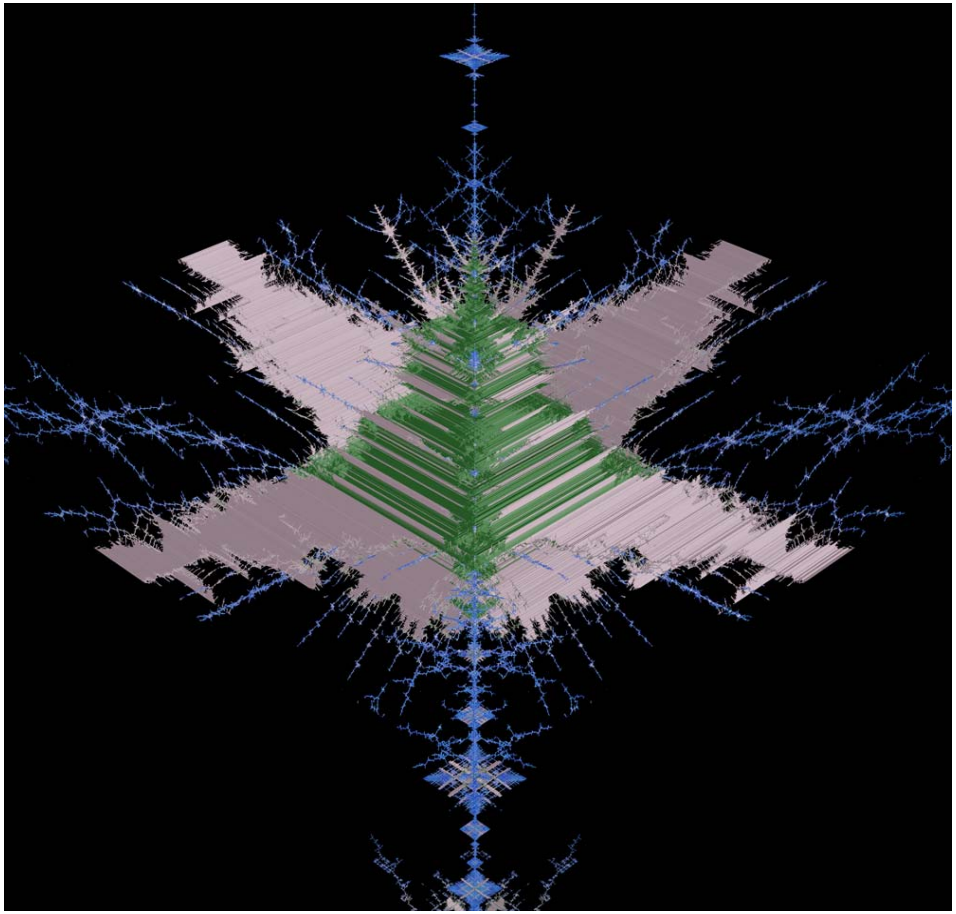

supplement

Tantrabrot

Kalachakra mandala

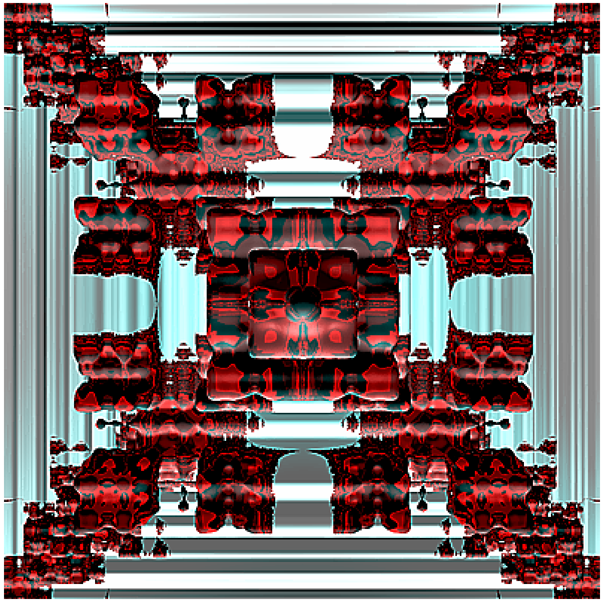

Tetrabrot from the top

supplement